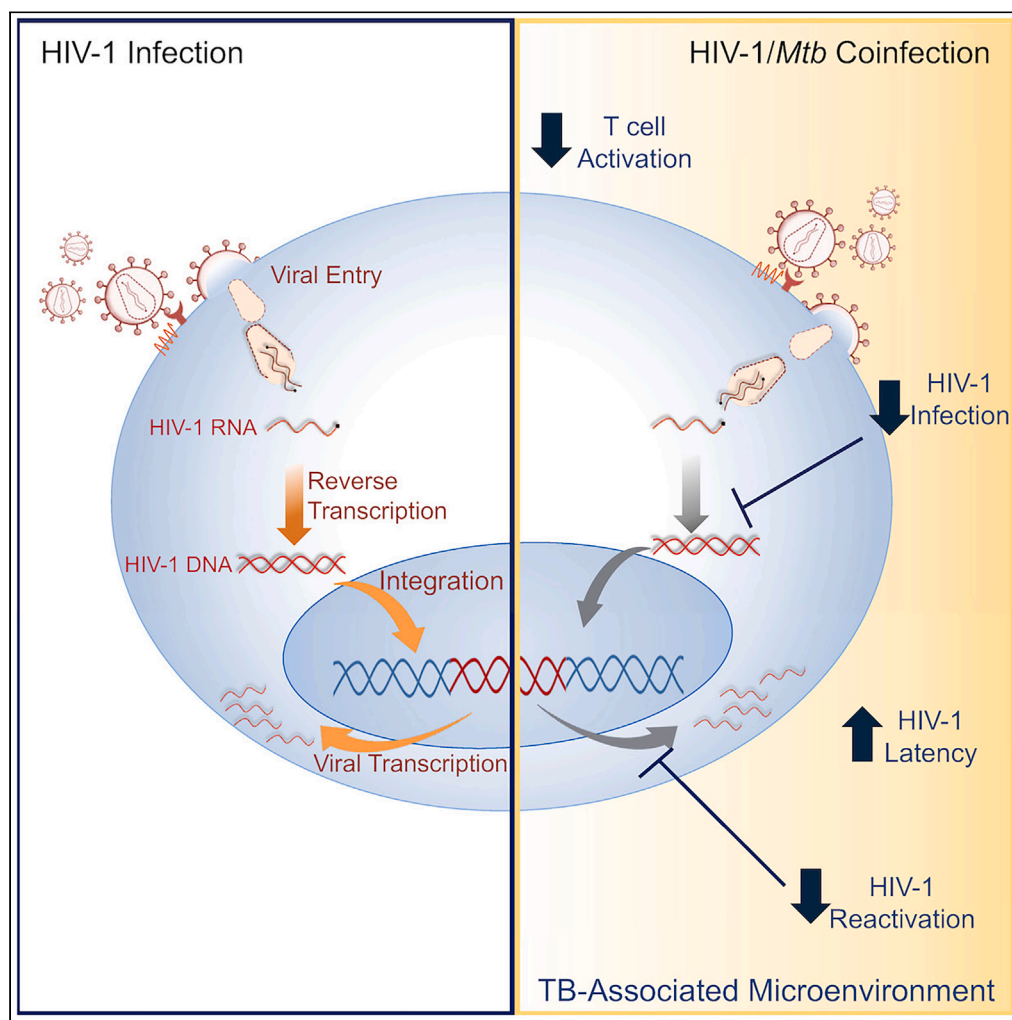Article

The immunosuppressive tuberculosis-associated microenvironment inhibits viral replication and promotes HIV-1 latency in CD4+ T cells

Samantha Cronin, Anneke de Vries-Egan, Zoï Vahlas, ..., Luciana Balboa, Sarah Palmer, Gabriel Duette

gabriel.duette@sydney.edu.au

Highlights

Tuberculous pleural effusion (TB-PE) inhibits HIV-1 replication in CD4+ T cells

This TB-associated microenvironment promotes HIV-1 latency

TB-PE inhibits HIV-1 reactivation in CD4+ T cells from people living with HIV-1

Article

The immunosuppressive tuberculosis-associated microenvironment inhibits viral replication and promotes HIV-1 latency in CD4+ T cells

Samantha Cronin,[1,2,8] Anneke de Vries-Egan,[1,8] Zoï Vahlas,[3,4] Alejandro Czernikier,[5] Claudia Melucci,[5] Pehuén Pereyra Gerber,[6] Thomas O'Neil,[1,2] Brian Gloss,[1] Mayssa Sharabas,[1] Gabriela Turk,[5] Christel Verollet,[3,4] Luciana Balboa,[4,5,7,9] Sarah Palmer,[1,2,9] and Gabriel Duette[1,2,9,10,*]

SUMMARY

***Mycobacterium tuberculosis* (*Mtb*), the causative agent of tuberculosis (TB), is the most common coinfection among people living with HIV-1. This coinfection is associated with accelerated HIV-1 disease progression and reduced survival. However, the impact of the HIV-1/TB coinfection on HIV-1 replication and latency in CD4+ T cells remains poorly studied.**

Using the acellular fraction of tuberculous pleural effusion (TB-PE), we investigated whether viral replication and HIV-1 latency in CD4+ T cells are affected by a TB-associated microenvironment. Our results revealed that TB-PE impaired T cell receptor-dependent cell activation and decreased HIV-1 replication in CD4+ T cells. Moreover, this immunosuppressive TB microenvironment promoted viral latency and inhibited HIV-1 reactivation.

This study indicates that the TB-induced immune response may contribute to the persistence of the viral reservoir by silencing HIV-1 expression, allowing the virus to persist undetected by the immune system, and increasing the size of the latent HIV-1 reservoir.

INTRODUCTION

Despite decades of research and the effectiveness of antiretroviral therapy (ART), HIV-1 remains an incurable infection. Globally in 2022, there were more than 38 million people living with HIV-1 (PLWH), with 630,000 individuals dying from HIV-1-related causes.[1] The major obstacle to an HIV-1 cure is the latent HIV-1 reservoir, as replication-competent HIV-1 proviruses persist within long-lived memory CD4+ T cells of ART-suppressed individuals.[2–6] These proviruses are largely transcriptionally silent and hence remain hidden from immune surveillance and CD8+ T cell-mediated clearance. However, the virus can rebound from these latently HIV-infected cells when ART is interrupted.[7–10]

A potential curative strategy for HIV-1 is called "shock and kill", which involves reactivation of HIV-1 from latently infected cells (shock) and subsequent elimination (killing) of these cells, through the combined effects of HIV-1-specific cytotoxic CD8+ T cells and ART.[11] Therefore, the success of these curative strategies in clearing HIV-1 from PLWH relies on the ability to broadly reactivate HIV-1 from latently infected cells.

Mycobacterium tuberculosis (*Mtb*), the causative agent of tuberculosis (TB), ranks alongside HIV-1 as a leading infectious killer. Over 10 million new cases of TB were identified in 2021, with a total of 1.6 million deaths attributed to TB infection.[12] In addition, an estimated one-third of HIV-1-infected individuals are coinfected with *Mtb*, with PLWH being 18 times more likely to develop active TB disease than HIV-1-negative individuals.[12] Importantly, PLWH and TB experience accelerated HIV-1 disease progression and reduced survival in comparison to people living with HIV-1 alone.[12,13] As such, TB remains the leading cause of death among PLWH, with 187,000 deaths attributed to HIV-1/TB coinfection in 2021—accounting for one in three acquired immunodeficiency syndrome (AIDS)-related deaths.[12,14]

It has been previously shown that infection with *Mycobacterium tuberculosis* (*Mtb*) or mycobacterial component(s) may promote HIV-1 replication.[15–21] Moreover, it has recently been demonstrated that TB-associated microenvironments, such as therapeutically aspirated

[1]The Westmead Institute for Medical Research, Centre for Virus Research, Westmead, NSW 2145, Australia
[2]University of Sydney, Faculty of Medicine and Health, Sydney, NSW 2050, Australia
[3]Institut de Pharmacologie et Biologie Structurale (IPBS), Université de Toulouse, Centre National de La Recherche Scientifique, Université Toulouse III - Paul Sabatier (UPS), 31077 Toulouse, France
[4]International Research Project CNRS "MAC-TB/HIV", Toulouse, France and Buenos Aires, Argentina
[5]Instituto de Investigaciones Biomédicas en Retrovirus y SIDA, Universidad de Buenos Aires-CONICET, Buenos Aires C1121ABG, Argentina
[6]Cambridge Institute for Therapeutic Immunology and Infectious Disease, Jeffrey Cheah Biomedical Centre, Cambridge CB2 0AW, UK
[7]Instituto de Medicina Experimental-CONICET, Academia Nacional de Medicina, Buenos Aires C1425ASU, Argentina
[8]These authors contributed equally
[9]Senior author
[10]Lead contact
*Correspondence: gabriel.duette@sydney.edu.au
https://doi.org/10.1016/j.isci.2024.110324

pleural effusions (PEs) from TB patients (TB-PE), render human macrophages highly susceptible to *Mtb* infection,[22,23] as well as to HIV-1 infection and spread.[21,24] However, contradictory evidence has also emerged showing inhibition of HIV-1 replication by *Mtb*, blurring our understanding of the interaction between these two pathogens.[25,26] Furthermore, whether *Mtb* influences viral replication and/or HIV-1 latency, specifically in CD4+ T cells, remains unclear.

Pleural effusion is an excess of fluid recovered from the pleural space of the human respiratory compartment and is found in approximately 30% of TB patients.[27] This excess of fluid is caused by the spread of *Mtb* into the pleural space, leading to subsequent local inflammation and leukocyte infiltration.[28] Importantly, in HIV-1/TB coinfected persons, the formation of PE is more common and contains high HIV-1 titers, compared to serum from the same individual.[29–31] Thus, TB-PE is a physiologically relevant fluid that can be used as an *ex vivo* model for a human compartment impacted by *Mtb* infection.[21,22,24,32] Therefore, in this study, we investigate the effects of TB-PE on viral replication and HIV-1 latency in CD4+ T cells.

RESULTS

Exposure to TB pleural effusion inhibits HIV-1 replication in primary CD4+ T cells

Whether the inflammatory microenvironment generated by the host immune response to *Mtb* infection impacts HIV-1 replication in CD4+ T cells remains undetermined. To address this question, primary CD4+ T cells were incubated with 20% v/v TB-PE (pooled from 9 participants with TB and devoid of viable mycobacteria) for 1–2 h and then infected with HIV-1. TB-PEs were obtained by therapeutic thoracentesis from patients who developed pleural effusion and were diagnosed with tuberculous pleurisy (see STAR Methods section). The proportion of infected cells was determined by HIV-1-p24 staining and flow cytometry at day 3 post-infection (Figure 1A). Of note, we did not observe significant differences in cell viability across the different treatments (Figure 1B). We found that the pre-treatment with TB-PE significantly decreased the proportion of HIV-1 infected cells in primary CD4+ T cells, as shown in Figure 1C. Importantly, this result was reproduced when cells were treated with TB-PE collected from two individual TB patients (Figure 1D). In contrast, pre-treatment with PE from individuals who experienced heart failure (HF-PE; pooled from 4 patients with transudates resulting from heart failure) did not exhibit a significant inhibition of HIV-1 infection, indicating that the inhibition of HIV-1 replication is dependent on the PE etiology (Figure 1E). Our results show that the TB microenvironment decreases HIV-1 replication in CD4+ T cells.

HIV-1 reverse transcription and integration, but not viral entry, are inhibited by exposure of CD4+ T cells to TB pleural effusion

To identify which steps of the viral replication cycle were affected by a TB-associated microenvironment, we used the BlaM-Vpr fusion assay to assess viral entry in primary CD4+ T cells pretreated with TB-PE.[33,34] A shift in the CCF2 fluorescence emission spectrum from 520 nm to 447 nm indicates the enzymatic cleavage of CCF2 by Vpr-BlaM and therefore viral fusion with the plasma membrane of CD4+ T cells. Pre-incubation with TB-PE did not exhibit significant differences in the entry of HIV-1 when compared to the control condition (Figure 1F). Next, we quantified the levels of reversed-transcribed viral DNA to evaluate the effect of TB-PE on HIV-1 reverse transcription. Intriguingly, we observed that the reverse transcription of viral DNA was significantly decreased by TB-PE treatment (Figure 1G). To determine whether the inhibition of the viral reverse transcription by TB-PE has an impact in the integration of the viral DNA into the host genome, we quantified HIV-1 integration by quantitative PCR (qPCR). In line with a decrease in the reverse transcription of viral DNA, the treatment with TB-PE results in lower levels of integrated HIV-1 (Figure 1H). These findings indicate that the microenvironment induced by *Mtb* infection impairs the replication of HIV-1 in CD4+ T cells by inhibiting viral reverse transcription and integration.

Transcriptional profile of CD4+ T cells exposed to TB pleural effusion

To understand the effect of the immune response to TB on CD4+ T cells and its potential impact on HIV-1 replication, we assessed the transcriptional profile of primary CD4+ T cells treated with TB-PE. Bulk RNA sequencing (RNA-seq) was performed on primary CD4+ T cells isolated from 3 healthy donors and treated with TB-PE. In addition, since T cell activation increases CD4+ T cells susceptibility to HIV-1 infection,[35] we also investigated the impact of TB-PE on CD4 T cells activated by anti-CD3/CD28 antibodies. As expected, the activation with anti-CD3/CD28 antibodies significantly changed the transcriptional profile of the stimulated CD4+ T cells as revealed by principal component analysis (PCA) (Figure 2A). Although PCA did not show consistent clustering patterns between untreated cells and cells incubated with TB-PE (Figure 2A), activated cells and TB-PE-treated activated cells clustered separately (Figure 2A). This result was further supported by the analysis of differentially expressed genes (DEGs) (Figures 2B and 2C; Table S2). Moreover, gene set enrichment analysis (GSEA) revealed that cellular pathways involved in T cell activation were downmodulated by TB-PE treatment in anti-CD3/CD28-stimulated cells (Figures 2D and 2E; Table S3).

To validate our RNA-seq results, we measured the expression of the activation markers CD69, CD25, and HLA-DR on primary CD4+ T cells upon the stimulation with anti-CD3/CD28 antibodies, in the presence or absence of TB-PE by flow cytometry. Consistent with our RNA-seq analysis, TB-PE treatment resulted in a significant decrease in the surface expression of these activation markers (Figure 2F). A decrease in T cell activation was also observed when the CD4+ T cells were treated with individual TB-PE samples from two TB patients (Figure 2G). However, no significant inhibition of T cell activation was exhibited when these cells were incubated with HF-PE (Figure 2G). This result indicates that T cell activation can be downmodulated specifically by this TB-associated microenvironment. Our analysis shows that the TB-associated microenvironment, induced by the host anti-*Mtb* immune response, results in immunosuppressive properties that lead to the downmodulation of the transcriptomic profile associated with T cell activation of CD4+ T cells.
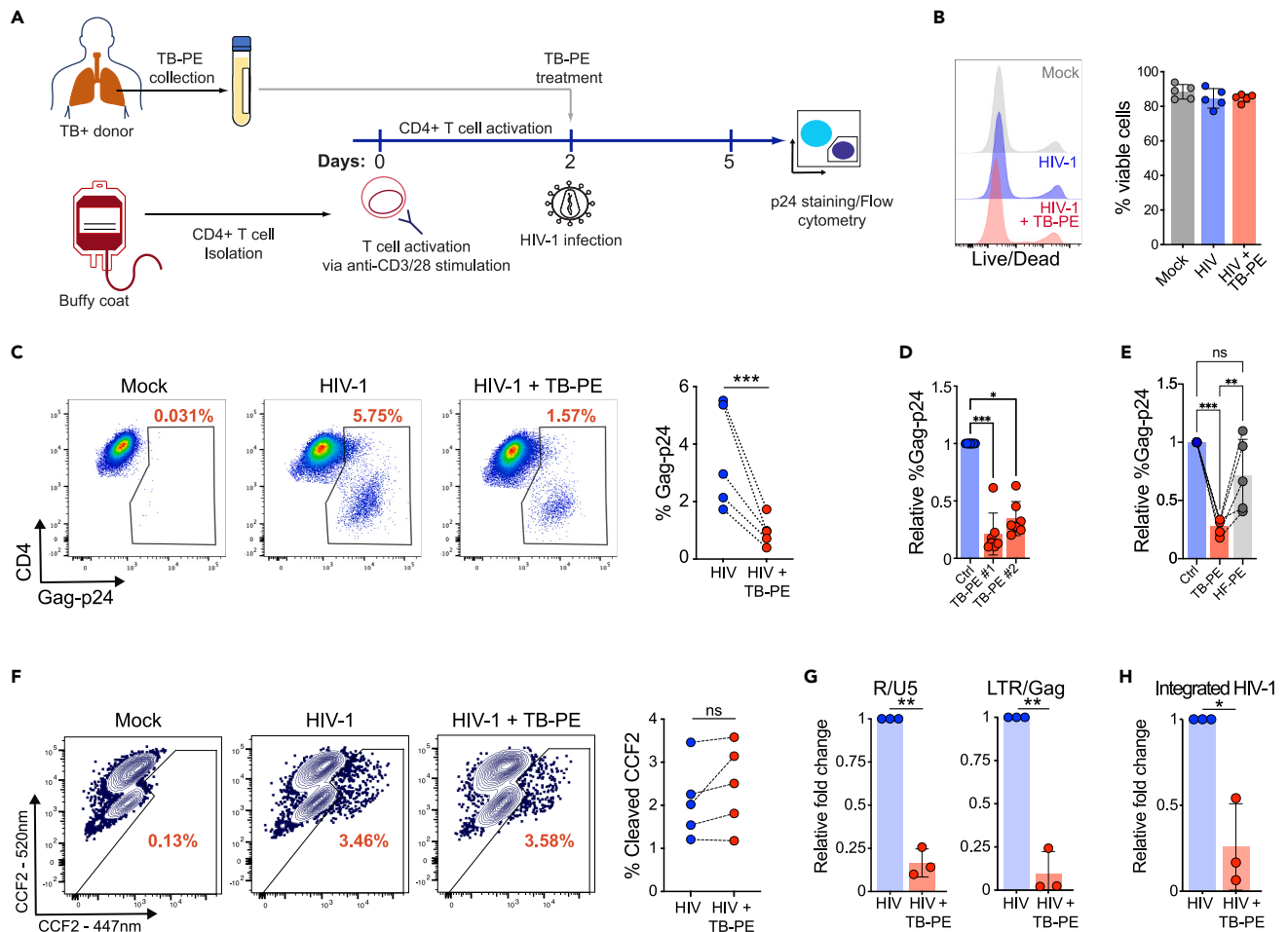
Figure 1. HIV-1 infection is inhibited by TB-PE in primary CD4+ T cells

Primary CD4+ T cells isolated from healthy donors were infected with HIV-1 in the presence of the acellular fraction of TB-PE. Cells infected with HIV-1 in the absence of TB-PE were used as a control.

(A) Schematic representation of the experimental design.

(B) Cell viability assessed by live/dead staining.

(C) The proportion of HIV-1 infected cells was determined at day 3 post-infection by Gag-p24 immunostaining. A representative cytometry (left) and Gag-p24 quantification (right) in cells from 5 independent donors are shown.

(D) Isolated CD4+ T cells from 7 healthy donors were infected with HIV-1 in the presence of TB-PE from 2 independent TB patients. The quantification of Gag-p24 positive cells, relative to HIV-1-infected cells in the absence of TB-PE, is shown.

(E) CD4+ T cells were treated with TB-PE or HF-PE and infected with HIV-1. The quantification of Gag-p24 positive cells relative to the control condition is shown.

(F) Viral entry was assessed by the HIV-1/BlaM-Vpr fusion assay. Enzymatic cleavage of CCF2 by BlaM-Vpr shifts the CCF2 fluorescence emission spectrum from 520 nm to 447 nm, indicating viral uptake.

(G) The HIV-1 reverse transcripts R/U5 and LTR/Gag were quantified by real-time qPCR at 6 h post-infection.

(H) Integrated HIV-1 DNA was measured by real-time qPCR at 24 h post-infection. Each dot represents values obtained from an independent donor. Data are represented as mean ± SD. Statistical significance was determined by paired two-tailed t test or One-way ANOVA followed by the Tukey's HSD post- test. $*p \leq 0.05$, $**p \leq 0.01$, $***p \leq 0.001$.

Oxidative phosphorylation and glycolysis are downregulated by TB pleural effusion treatment

Since T cell receptor (TCR)-mediated activation increases the levels of glycolysis and oxidative phosphorylation (OXPHOS) in CD4+ T cells, and as these two metabolic pathways are necessary for efficient HIV-1 replication,[36–38] we also analyzed the metabolic profile of TB-PE-treated CD4+ T cells. We used the ATP rate assay and a Seahorse cell flux analyzer to measure oxygen consumption rate (OCR) and the proton efflux rate (PER) in CD4+ T cells as indicators of OXPHOS and glycolysis, respectively. The intracellular rate of ATP production derived from glycolysis (glycoATP) or OXPHOS (mitoATP) was also quantified. In line with the observed inhibition of T cell activation, both OXPHOS and glycolysis levels were significantly lower in TB-PE-treated cells when compared to controls (Figures 3A and 3B). Importantly, the incubation with HF-PE did not significantly impact either glycolysis or OXPHOS, indicating that this effect is specific to the TB-associated microenvironment.
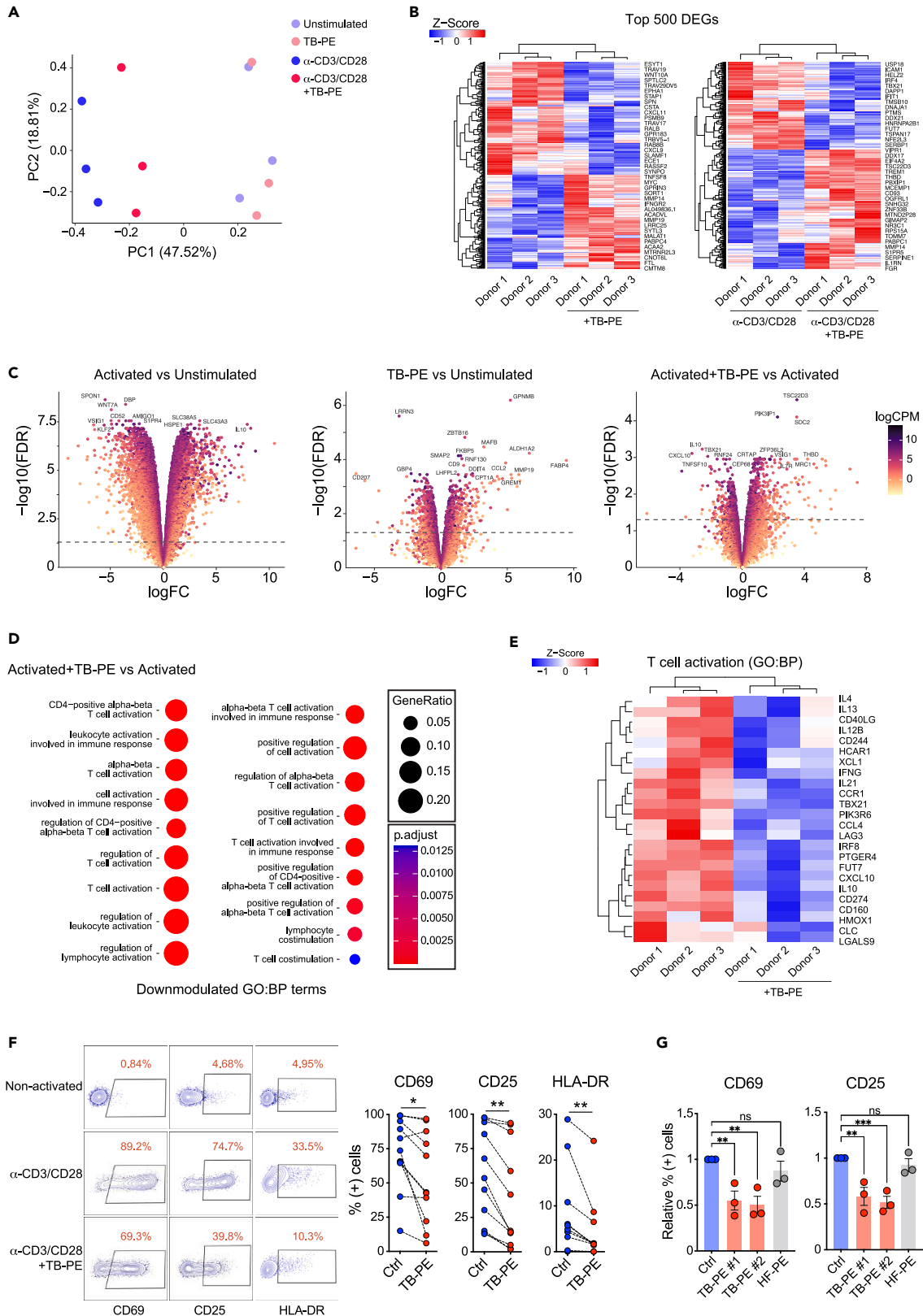
Figure 2. Transcriptional profile of CD4⁺ T cells exposed to TB-PE

The transcriptional profile of primary CD4⁺ T cells treated with TB-PE was characterized by bulk RNA-seq analysis in resting and activated cells from 3 healthy donors.

(A) Principal component analysis of resting and activated CD4⁺ T cells.

(B) Heatmaps displaying hierarchical clustering of the top 500 variable genes between TB-PE-treated and control CD4⁺ T cells. Data from resting (left) and activated (right) CD4⁺ T cells are shown.

(C) Volcano plots representing the differentially expressed genes (DEGs) analysis.

(D) Gene set enrichment analysis (GSEA) comparing TB-PE-treated and control CD4⁺ T cells in resting and activated cells (DEGs: FDR<0.05 and absolute logFC>1). Dot plots illustrating the enriched GO biological processes terms related to T cell activation. The size of the dot reflects the gene ratio, indicating the proportion of differentially expressed genes associated with the pathway. The color intensity of the dot corresponds to the significance of enrichment, as determined by the adjusted p value.

(E) Heatmaps displaying the normalized expression of specific genes involved in T cell activation. Primary CD4⁺ T cells were stimulated with anti-CD3/CD28 antibodies in the presence of TB-PE or HF-PE. Cells activated in the absence of PEs were used as control.

(F) The expression of the activation markers CD69, CD25 and HLA-DR was measured by flow cytometry after 24 h (CD69 and CD25) or 48 h post-activation (HLA-DR). A representative cytometry (left) and the proportion of activated cells (right) are shown.

(G) Proportion of CD69 (left) or CD25 (right) positive cells stimulated in the presence of TB-PE from 2 independent TB-infected donors (red) or HF-PE (gray). Values are relative to the non-PE control condition (blue). Data are represented as mean $\pm$ SD. Each dot represents values obtained from an independent donor. Statistical significance was determined by paired two-tailed t test or one-way ANOVA followed by the Tukey's HSD post-test. *$p \leq 0.05$, **$p \leq 0.01$.

Since we and others have shown that the hypoxic inducible factor 1 alpha (HIF-1α) regulates and promotes glycolysis upon T cell activation and is also necessary for HIV-1 replication,[39] we quantified the expression of HIF-1α in CD4⁺ T cells. Interestingly, the treatment with TB-PE significantly inhibited the expression of HIF-1α in activated CD4⁺ T cells (Figure 3C). These results suggest that the microenvironment found at the site of the TB infection inhibits metabolic pathways and factors necessary for efficient HIV-1 replication in CD4⁺ T cells.

Cellular pathways involved in HIV-1 latency are modulated by TB pleural effusion treatment

The persistence of latently HIV-1 infected cells poses a significant barrier to eradicating the viral reservoir in PLWH. Therefore, we investigated the impact of the TB-associated microenvironment on HIV-1 latency in CD4⁺ T cells. Based on our RNA-seq data obtained from activated CD4⁺ T cells, we analyzed cellular pathways necessary for efficient HIV-1 transcription and viral reactivation of latently HIV-1-infected cells.[40–47] These cellular pathways include the nuclear factor kappa-light-chain-enhancer of activated B cells (NF-κB), Janus kinase/signal transducer and activator of transcription (JAK-STAT), tumor necrosis factor (TNF), extracellular signal-regulated kinases (ERK), and type I/II interferon (IFN) pathways.[40–47] We found that NF-κB, JAK-STAT, and type I/II IFN pathways were downmodulated in activated cells treated with TB-PE (Figures 4A and 4B). The NF-κB and type I/II IFN pathways were also downmodulated by TB-PE in non-activated CD4⁺ T cells (Figure S1). Furthermore, we observed upregulation of pathways associated with transforming growth factor β (TGFβ)-SMAD response, which is known to support HIV-1 latency,[47–49] in the cells exposed to TB-PE (Figures 4A and 4B). Of note, regulation of the ERK cascade signaling did not show consistent modulation patterns (Figure 4A). We also analyzed the expression of genes and pathways associated with programmed cell death, since previous studies indicate that intrinsic resistance to cell death of CD4⁺ T cells that compose the long-lived latent viral reservoir may contribute to HIV-1 persistence.[47,50–53] Our analysis revealed that programmed cell death pathways are inhibited by TB-PE (Figure S2A). This result was further validated by measuring the proportion of dead cells in CD4⁺ T cells treated with TB-PE after two days of cell activation (Figure S2B). This finding suggests that CD4⁺ T cells exposed to TB-PE are less susceptible to cell death, which in turn could promote the persistence of latently HIV-1-infected cells.

TB pleural effusion increases the proportion of latently HIV-1 infected CD4⁺ T cells

Several research groups have developed viral vectors containing the HIV-1 genome encoding a fluorescent reporter protein under the control of the viral LTR alongside a second reporter protein under the transcriptional control of an LTR-independent promotor.[54–57] This strategy allows for the identification of latently and productively infected cells. Applying this strategy, we developed a dual HIV-1 latency reporter encoding two reporter proteins: the green fluorescent protein (GFP) and near-infrared fluorescent protein (iRFP) (Figure 4C). In our reporter HIV-1 construct, the expression of GFP is under the control of the viral LTR while iRFP expression is regulated by the spleen focus forming virus promoter (SFFV). We selected this promoter since SFFV is known to provide high-level transgene expression in primary human CD4⁺ T cells.[58,59] To test our new viral reporter of HIV-1 latency, we infected the CD4⁺ T cell line CEM, and measured the expression of GFP and iRFP by flow cytometry. The infection of CEM T cells with our dual reporter virus resulted in three populations: double-positive for GFP and iRFP (productively infected cells), single-positive for iRFP (latently infected cells), and double-negative for both reporter proteins (uninfected bystander cells) (Figure 4D). To functionally validate our reporter virus, we assessed the expression of CD4 and tetherin in the three populations. Since these two surface proteins are degraded by the viral protein Vpu, they should therefore be downmodulated in productively HIV-1-infected cells but not by cells latently infected with our reporter virus.[60] As expected, GFP+iRFP+ cells efficiently downmodulated the expression of both CD4 and tetherin (Figure 4D). However, iRFP+ cells expressed both markers at similar levels as bystander cells (Figure 4D) confirming a latent infection. After validating our reporter system of HIV-1 latency, we evaluated whether TB-PE increases the proportion of latently HIV-1 infected T cells. For this experiment, Jurkat CD4⁺ T cells were infected with our dual HIV-1 latency reporter in the presence or absence of TB-PE and the proportion of latently vs. productively infected cells was analyzed within the HIV-1 infected cell population. Remarkably, the treatment with TB-PE increased the proportion of latently infected cells and reduced the proportion of productively
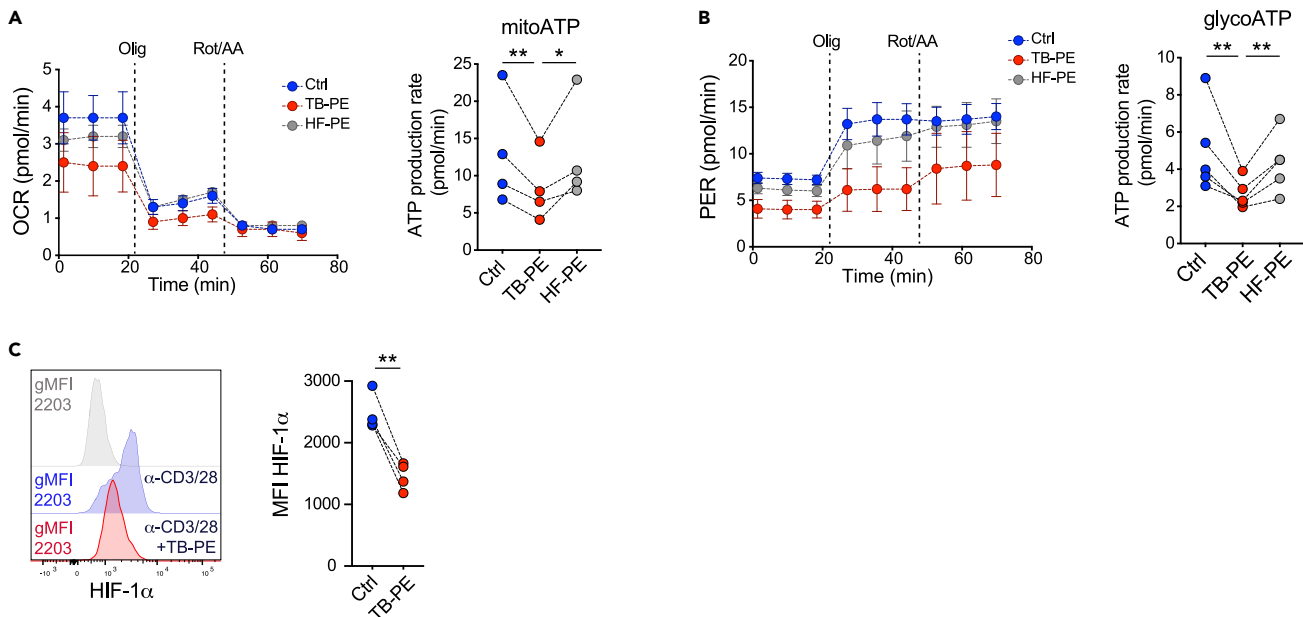
Figure 3. TB-PE decreases glycolysis and oxidative phosphorylation
Primary CD4$^+$ T cells were stimulated with anti-CD3/CD28 antibodies in the presence of TB-PE or HF-PE. Cells activated in the absence of PEs were used as control.
(A) Oxidative phosphorylation determined by oxygen consume rate (OCR, left) and mitochondrial-dependent ATP production rate (right).
(B) Level of glycolysis was determined by proton efflux rate (PER, left) and glycolysis-dependent ATP production rate (right).
(C) HIF-1α expression in activated CD4$^+$ T cells was determined by flow cytometry. Each dot represents values obtained from an independent donor. Statistical significance was determined by paired two-tailed t test or One-way ANOVA followed by the Tukey's HSD post-test. *$p \leq 0.05$, **$p \leq 0.01$.

infected cells (Figures 4E and S3A–S3C). Importantly, this result was reproduced when primary CD4$^+$ T cells were infected with our dual HIV-1 latency reporter (Figures 4F and S3D–S3F). Next, we evaluated whether treatment with TB-PE promotes HIV-1 latency by inhibiting viral transcription after the integration of the HIV-1 genome. Since HIV-1 completes its replication cycle in approximately 24 h,[61] primary CD4$^+$ T cells were treated with TB-PE 24 h post-infection and GFP expression was measured at day 3 post-infection. We observed that the treatment with TB-PE led to a lower proportion of productively infected cells, indicating that post-integration HIV-1 transcription is decreased by TB-PE (Figure S3G). Our findings indicate that the TB microenvironment promotes HIV-1 latency in CD4$^+$ T cells.

Reversal of HIV-1 latency is inhibited by TB pleural effusion treatment
Since our results showed that TB-PE promotes HIV-1 latency, we hypothesized that reactivation of latent HIV-1 may be impaired by this TB-associated microenvironment. To address our hypothesis, we used the J-Lat latency model. These Jurkat-derived cell lines are clones of cells containing one copy of integrated HIV-1 encoding the reporter GFP. Upon stimulation with latency reversing agents (LRAs) these cells express GFP, allowing for the quantification of HIV-1 reactivation by flow cytometry. To determine whether TB-PE affects the reactivation of latent HIV-1, we treated J-Lat cells (clones 6.3 and 10.6) with phorbol 12-myristate 13-acetate (PMA), a potent and well characterized LRA, in the presence or absence of TB-PE. In line with our previous results, the incubation with TB-PE inhibited the expression of GFP by both J-Lat clones (Figures 5A and 5B). The reactivation of HIV-1 was also inhibited when the cells were stimulated with latency reversal agents ingenol-3-angelate (PEP005) (both J-Lat clones; Figures 5A and 5B) and JQ1 (J-Lat clone 10.6; Figure 5B). Interestingly, TB-PE did not inhibit the reversal of HIV-1 latency induced by TNF-α (both J-Lat clones; Figures 5A and 5B) and vorinostat (J-Lat clone 10.6; Figure 5B), indicating that TB-PE inhibition is pathway-specific. Of note, JQ1 and vorinostat were used only on J-Lat clone 10.6 due to the cytotoxic effect of these LRAs on J-lat clone 6.3 (Figure S4).

Finally, to validate our in vitro results, we evaluated the effect of TB-PE ex vivo on cells obtained from PLWH. Isolated CD4$^+$ T cells from 3 HIV-1-positive donors on ART were treated with PMA in the presence or absence of TB-PE. Levels of viral reactivation were quantified by measuring unspliced (US) HIV-1 RNA by quantitative PCR (qPCR). In agreement with our in vitro results, the incubation with TB-PE significatively inhibited viral reactivation of HIV-1 ex vivo (Figure 5C). Altogether, our results indicate that this TB-associated microenvironment induces viral latency and inhibits the reactivation of HIV-1 in latently infected CD4$^+$ T cells.

DISCUSSION
While a growing body of evidence indicates worsened clinical outcomes in individuals coinfected with HIV-1 and *Mtb*, the precise interaction between these two pathogens remains unclear.[62] The immunological interplay between HIV-1 and *Mtb* has predominantly focused on the
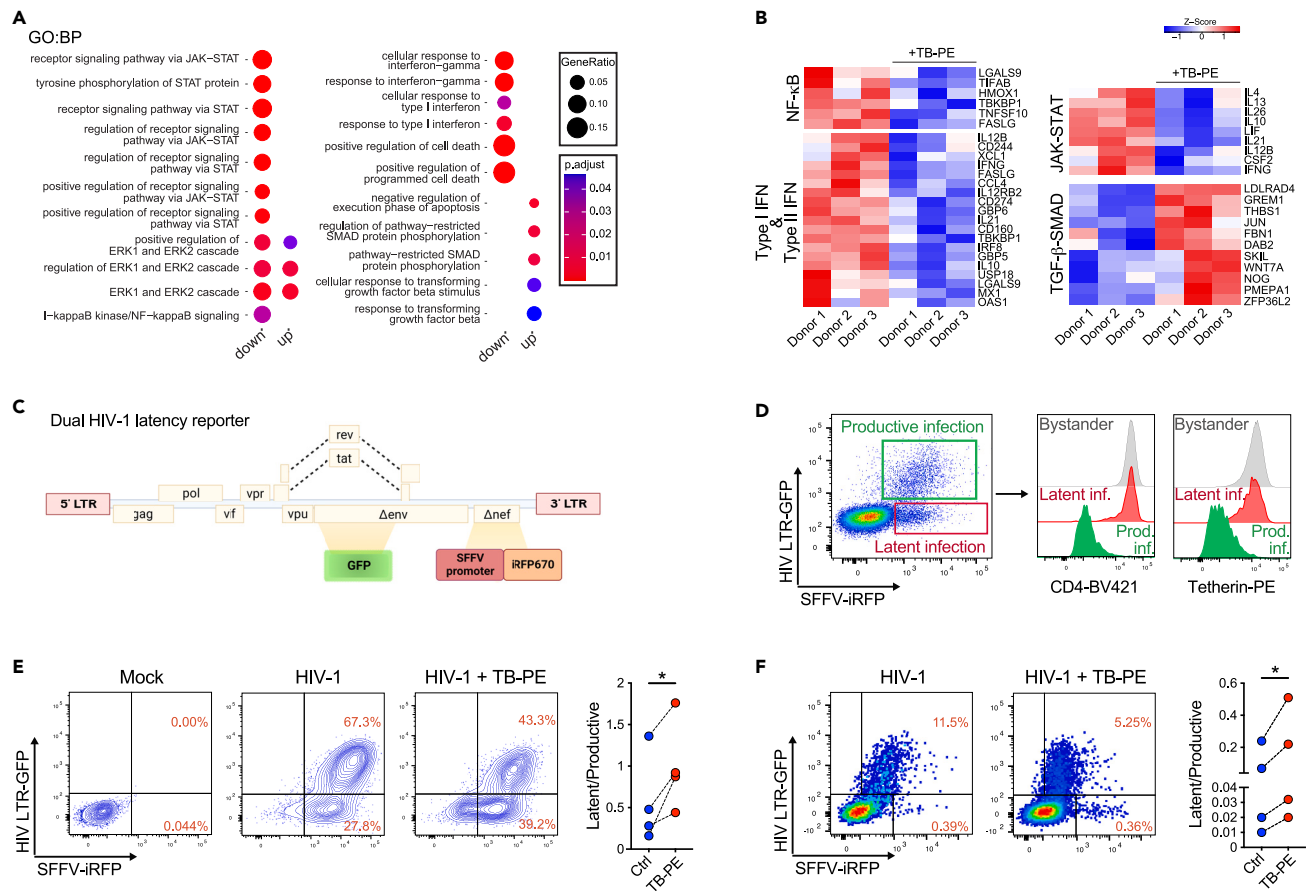
Figure 4. TB-PE promotes latency in CD4+ T cells

(A) Gene set enrichment analysis (GSEA) comparing TB-PE-treated and control CD4+ T cells in activated cells (DEGs: FDR<0.05 and absolute logFC>1). The dot plots illustrate the positively and negatively enriched GO biological processes terms involved in HIV-1 transcription and reactivation. The size of the dot reflects the gene ratio, indicating the proportion of differentially expressed genes associated with the pathway. The color intensity of the dot corresponds to the significance of enrichment, as determined by the adjusted p value.

(B) Heatmaps displaying the normalized expression of specific genes involved in cellular pathways necessary for HIV-1 transcription and reactivation.

(C) Schematic of the dual HIV-1 latency reporter construct.

(D) CEM CD4+ T cells were infected with the dual HIV-1 latency reporter and the proportion productively (GFP+/iRFP+) and latent (iRFP+) infected cells was determined by flow cytometry (left). The expression of CD4 (middle) and tetherin (right) on each gated population is shown. Jurkat (E) or primary CD4+ T cells (F) were infected with the dual HIV-1 latency reporter virus in the presence or absence of TB-PE. Representative cytometry (left) and the ratio between latent and productively infected cells (right) are shown. Each dot represents values obtained from an independent experiment (E) or independent donor (F). Statistical significance was determined by paired two-tailed t test *$p \leq 0.05$. See also Figures S1–S3.

virus-driven exacerbation of tuberculosis pathogenesis.[63] However, our understanding of the mechanisms underlying the influence of pre-existing or subsequent *Mtb* infection on the replication, persistence, and progression of HIV-1, particularly in CD4+ T cells, is limited and requires further characterization. In this study, we investigated how a TB-associated microenvironment impacts HIV-1 infection and latency in CD4+ T cells. To further understand the interaction between both pathogens, in our study, we use pleural effusion from TB patients, which reflects the microenvironment induced by *Mtb* infection and represents a relevant model for studying interactions at the site of the coinfection.[21,23,32,64]

Here, we show that TB-PE decreases HIV-1 replication in CD4+ T cells by inhibiting early steps in the HIV-1 replication cycle, the reverse transcription and integration of the viral genome. These results contrast with previous publications showing that TB-associated microenvironments or mycobacterial components increase HIV-1 replication and spread.[19,21,24,26,65,66] However, these studies have investigated HIV-1 replication in macrophages, indicating that the effect of *Mtb* infection and the TB-associated microenvironment varies between cell types.[19,21,24,26,65,66] Nevertheless, one study has shown that *Mtb* infection can also inhibit HIV-1 infection in monocyte-derived macrophages.[25] Of note, He et al. have shown that blood-derived CD4+ T cells from individuals latently infected with *Mtb* supported HIV-1 replication more efficiently.[67] Importantly, the authors did not detect this increase in viral infectivity when HIV-1 infection was assessed in cells from individuals undergoing active TB, which is when TB-PE is observed.[67] The contrasting findings from these studies highlight the complexity of the HIV-1/TB interaction.
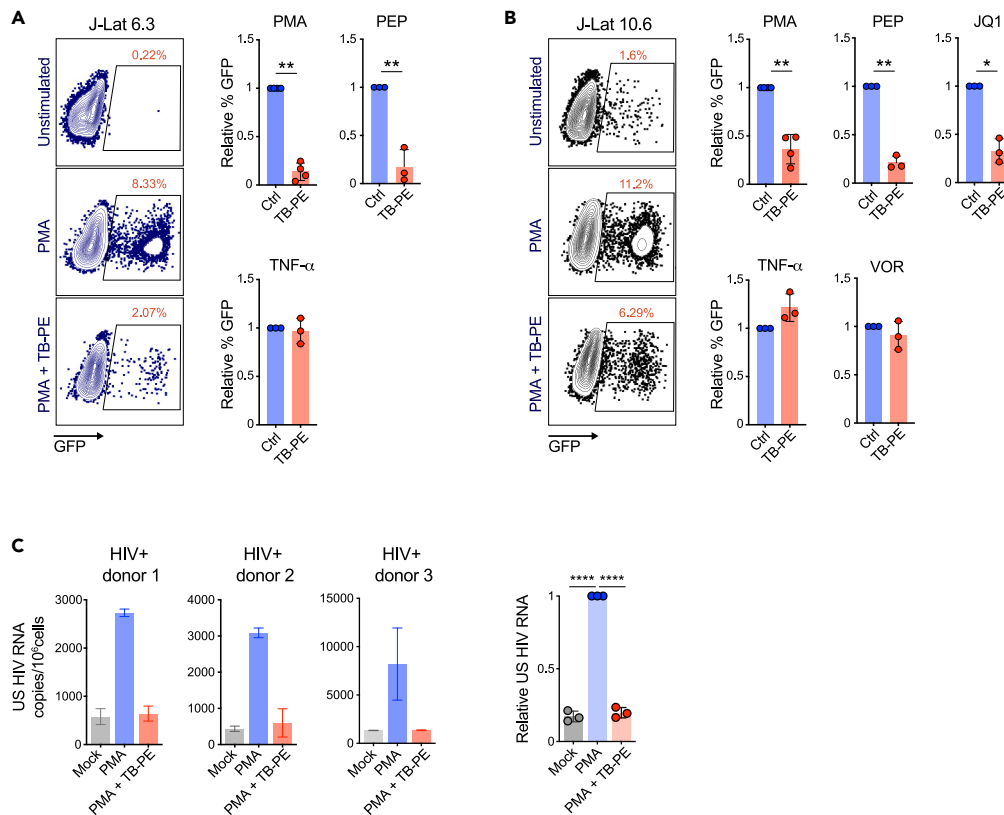
Figure 5. Reversal of HIV1 latency is impaired by TB-PE

J-Lat 6.3 (A) and 10.6 (B) cells were treated with different LRAs for 48 h in the presence or absence of TB-PE and GFP expression was measured by flow cytometry as a correlate for viral reactivation. A representative cytometry (left) and GFP quantification relative to the control condition (right) are shown.

(A) J-Lat 6.3 cells were treated with 2 ng/ml PMA, 50 nM PEP005 or 10 ng/mL TNF-α.

(B) J-Lat 10.6 cells were treated with 0.5 ng/mL PMA, 0.05 ng/mL TNF-α, 5nM PEP005, 1μM JQ1, or 10μM vorinostat. Each dot represents values obtained from an independent experiment. Statistical significance was determined by paired two-tailed t test.

(C) Unspliced HIV-1 RNA (US HIV RNA) was measured in CD4$^+$ T cells from 3 HIV-1-infected donors on ART after the stimulation with 2 ng/ml PMA. Values obtained by real-time qPCR (left) and relative quantification of US HIV RNA copies per 10^6 cells (right) are shown. Each dot represents values obtained from an independent donor. Data are represented as mean $\pm$ SD. Statistical significance was determined by One-way ANOVA followed by the Tukey's HSD post-test. *$p \leq 0.05$, **$p \leq 0.01$, ****$p \leq 0.0001$. See also Figure S4.

As mentioned previously, the differences observed between our study and others can be explained in part by the cell type studied. In addition, our experimental model incorporates immune factors released in the microenvironment induced by *Mtb* infection. We observed that this microenvironment can modify the transcriptional profile of CD4$^+$ T cells, particularly when these cells undergo TCR-dependent activation. T cell activation and downstream cellular events, such as increased rate of glycolysis and OXPHOS, as well as the expression of the metabolic regulator HIF-1α, were drastically inhibited by TB-PE. This inhibition is consistent with the observed decrease in HIV-1 infection since these cellular pathways and factors are required for efficient HIV-1 replication in CD4$^+$ T cells.[35–39,68–71] In agreement with our results, it has been reported that immunosuppressive mediators present in pleural fluid from tuberculous pleurisy inhibit cytokine production, cell activation, and Th1 differentiation of CD4$^+$ T cells.[72] Although we have focused our research on the impact of this immune microenvironment on HIV-1 replication and latency, our results suggest that diminished CD4$^+$ T cell activation may also result in an impaired T cell-mediated immune response in coinfected individuals. This hypothesis is supported by the studies conducted by Chetty et al., where they observe that the co-infection with *Mtb* impairs HIV-1-specific CD8$^+$ and CD4$^+$ T cell functionality.[73] On the other hand, it has also been reported that TB disease associates with higher HIV-1-specific antibody responses,[74] indicating that the infection with *Mtb* does not impact all the components of the adaptive anti-HIV-1 immune response.

Even though a comprehensive understanding of viral latency is critical to progress toward an HIV-1 cure, the number of studies addressing this issue in the context of the HIV-1/TB coinfection remains limited to a few reports. For instance, recent studies have reported that components of the *Mtb* membrane and exosomes secreted by *Mtb*-infected macrophages reversed HIV-1 latency.[75,76] Moreover, it has also been shown that different mycobacterial components can modulate LTR-dependent transcription of HIV-1 in cell lines,[18,20] suggesting that these components may enhance HIV-1 transcription and reactivation. These reports contrast with our results showing that TB-PE promotes HIV-1

latency and impairs viral reactivation. However, as mentioned previously, differences in our experimental model may explain these contrasting results. Of note, Olson and colleagues have reported that TB disease is associated with inflammation and decreased HIV-1 RNA expression relative to the number of infected cells, indicating that the coinfection with *Mtb* may promote HIV-1 latency *in vivo*.[77] In line with the promotion of HIV-1 latency, our transcriptional profile analysis showed that cellular pathways necessary for HIV-1 transcription and reactivation, such as NF-κB and STAT,[41,42,44] are downregulated by the TB-associated microenvironment. In addition, the TGF-SMAD pathway, reported to support HIV-1 latency,[48,49] was upregulated. Importantly, a decrease in T cell activation, OXPHOS and glycolysis has also been associated with the establishment of HIV-1 latency,[47,78–80] supporting our hypothesis. Interestingly, we observed that cell apoptosis is downmodulated in TB-PE-treated activated cells, indicating that this microenvironment may promote the survival of latently infected cells contributing to the persistence of HIV-1.

Since our results indicate that the immunosuppressive microenvironment generated by *Mtb* infection promotes HIV-1 latency, we hypothesize that the reactivation of HIV-1 might be impaired by this microenvironment. Indeed, we observed that TB-PE inhibits HIV-1 latency reversal in the cell line J-Lat and in cells from PLWH. However, this inhibition was restricted to some of the LRAs used in this study. For instance, HIV-1 reactivation by the PKC activators PMA (in both J-Lat cells and cells from PLWH) and PEP005 were drastically affected by TB-PE. This result is in line with our previous observations since PKC signaling is necessary for the TCR-triggered activation of T cells, which is dysregulated by TB-PE.[81] In contrast, despite TB-PE treatment, HIV-1 latency was efficiently reversed by vorinostat, a histone deacetylase (HDAC) inhibitor, and TNF-α. This is consistent with the finding that TB-PE mainly disrupts the TCR-mediated cell activation axes. However, JQ1, whose epigenetic mechanism of HIV-1 reactivation is by inhibiting the BET (bromodomain and extra-terminal domain) bromodomain BRD4 (bromodomain-containing protein 4), was also affected by TB-PE. This indicates that additional pathways can also be inhibited by this TB-associated microenvironment beyond those directly associated with T cell activation. This result indicates that some LRAs may be less effective in HIV-1/TB coinfected individuals.

In conclusion, our results indicate that the immune response against *Mtb* infection leads to an anti-inflammatory microenvironment which promotes viral latency and persistence of HIV-1 at the site of the coinfection. While HIV-1 silencing mediated by this TB-associated microenvironment may reduce viral replication and spread at this specific anatomic site, its overall effect on the viral reservoir size may lead to negative clinical outcomes by stabilizing the HIV-1 reservoir and supporting its long-term persistence. Further research investigating the impact of the TB-associated microenvironment on the viral reservoir and anti-HIV-1 immune control is critical to complement and expand the findings of our study.

Limitations of the study

Although our study provides mechanistic insights on the impact of the HIV-1/TB-coinfection on HIV-1 replication and latency, our findings rely on *in vitro* experimental data. However, by using TB-PE as well as CD4$^+$ T cells obtained from people living with HIV-1, we have developed a physiologically relevant model for researching the complex interactions between HIV-1 and the TB immune response. Therefore, the outcomes from this model contribute to relevant initial observations about HIV-1 persistence in CD4$^+$ T cells in the context of HIV/TB coinfection. Another limitation is the use of lab-strain HIV-1 to study viral replication and latency. Hence, future research including primary strains of HIV-1 might be necessary to support the clinical relevance of our findings.

STAR★METHODS

Detailed methods are provided in the online version of this paper and include the following:

- KEY RESOURCES TABLE
- RESOURCE AVAILABILITY
  - Lead contact
  - Materials availability
  - Data and code availability
- EXPERIMENTAL MODEL AND STUDY PARTICIPANT DETAILS
  - Ethical statement
  - Participant cohort and clinical samples
  - Pleural effusion samples
  - Primary CD4$^+$ T cells and cell lines
  - Plasmids and HIV-1 viral strains
  - Preparation of viral stocks
- METHOD DETAILS
  - HIV-1 infection
  - Quantification of HIV-1 reverse transcripts
  - Quantification of integrated HIV-1 DNA
  - HIV-1 fusion assay
  - Dual HIV-1 latency reporter
  - RNAseq library

- ○ RNAseq analysis
- ○ *In vitro* reactivation of HIV-1
- ○ *Ex vivo* reactivation of HIV-1
- ○ Glycolysis and oxidative phosphorylation rate measurement
- ● QUANTIFICATION AND STATISTICAL ANALYSIS

AUTHOR CONTRIBUTIONS

G.D., L.B., and S.P. conceptualized and designed the study. S.C., A.V., and G.D. designed and conducted the majority of *ex vivo* and *in vitro* experiments. A.C. and G.T. evaluated *ex vivo* HIV reactivation. C.M. and P.P.G. developed the dual HIV-1 latency reporter. B.G. and T.O. contributed to the transcriptomic analysis. M.S. assisted with *in vitro* experiments. Z.V. and C.V. performed metabolic assays. G.D. wrote the original manuscript. S.C., L.B., and S.P. supervised and edited the original manuscript. Co-first authorship order was determined by the contribution to the results presented in the manuscript and contribution to writing the initial manuscript draft.

DECLARATION OF INTERESTS

The authors declare no competing interests.

REFERENCES

1. WHO (2022). HIV and AIDS Fact sheet. https://www.who.int/news-room/fact-sheets/detail/hiv-aids.

2. Chun, T.W., Stuyver, L., Mizell, S.B., Ehler, L.A., Mican, J.A., Baseler, M., Lloyd, A.L., Nowak, M.A., and Fauci, A.S. (1997). Presence of an inducible HIV-1 latent reservoir during highly active antiretroviral therapy. Proc. Natl. Acad. Sci. USA *94*, 13193–13197. https://doi.org/10.1073/pnas.94.24.13193.

3. Finzi, D., Hermankova, M., Pierson, T., Carruth, L.M., Buck, C., Chaisson, R.E., Quinn, T.C., Chadwick, K., Margolick, J., Brookmeyer, R., et al. (1997). Identification of a reservoir for HIV-1 in patients on highly active antiretroviral therapy. Science *278*, 1295–1300. https://doi.org/10.1126/science.278.5341.1295.

4. Palmer, S., Josefsson, L., and Coffin, J.M. (2011). HIV reservoirs and the possibility of a cure for HIV infection. J. Intern. Med. *270*, 550–560. https://doi.org/10.1111/j.1365-2796.2011.02457.x.

5. Wong, J.K., Hezareh, M., Günthard, H.F., Havlir, D.V., Ignacio, C.C., Spina, C.A., and Richman, D.D. (1997). Recovery of replication-competent HIV despite prolonged suppression of plasma viremia. Science *278*, 1291–1295. https://doi.org/10.1126/science.278.5341.1291.

6. Chomont, N., El-Far, M., Ancuta, P., Trautmann, L., Procopio, F.A., Yassine-Diab, B., Boucher, G., Boulassel, M.R., Ghattas, G., Brenchley, J.M., et al. (2009). HIV reservoir size and persistence are driven by T cell survival and homeostatic proliferation. Nat. Med. *15*, 893–900. https://doi.org/10.1038/nm.1972.

7. Duette, G., Hiener, B., Morgan, H., Mazur, F.G., Mathivanan, V., Horsburgh, B.A., Fisher, K., Tong, O., Lee, E., Ahn, H., et al. (2022). The HIV-1 proviral landscape reveals that Nef contributes to HIV-1 persistence in effector memory CD4+ T cells. J. Clin. Invest. *132*, e154422. https://doi.org/10.1172/JCI154422.

8. Hiener, B., Horsburgh, B.A., Eden, J.S., Barton, K., Schlub, T.E., Lee, E., von Stockenstrom, S., Odevall, L., Milush, J.M., Liegler, T., et al. (2017). Identification of Genetically Intact HIV-1 Proviruses in Specific CD4(+) T Cells from Effectively Treated Participants. Cell Rep. *21*, 813–822. https://doi.org/10.1016/j.celrep.2017.09.081.

9. De Scheerder, M.A., Vrancken, B., Dellicour, S., Schlub, T., Lee, E., Shao, W., Rutsaert, S., Verhofstede, C., Kerre, T., Malfait, T., et al. (2019). HIV Rebound Is Predominantly Fueled by Genetically Identical Viral Expansions from Diverse Reservoirs. Cell Host Microbe *26*, 347–358.e7. https://doi.org/10.1016/j.chom.2019.08.003.

10. Chun, T.W., Justement, J.S., Murray, D., Hallahan, C.W., Maenza, J., Collier, A.C., Sheth, P.M., Kaul, R., Ostrowski, M., Moir, S., et al. (2010). Rebound of plasma viremia following cessation of antiretroviral therapy despite profoundly low levels of HIV reservoir: implications for eradication. AIDS *24*, 2803–2808. https://doi.org/10.1097/QAD.0b013e328340a239.

11. Pham, H.T., and Mesplède, T. (2018). The latest evidence for possible HIV-1 curative strategies. Drugs Context *7*, 212522. https://doi.org/10.7573/dic.212522.

12. WHO (2022). Tuberculosis Fact Sheet. https://www.who.int/news-room/fact-sheets/detail/tuberculosis.

13. Whalen, C., Horsburgh, C.R., Hom, D., Lahart, C., Simberkoff, M., and Ellner, J. (1995). Accelerated course of human immunodeficiency virus infection after tuberculosis. Am. J. Respir. Crit. Care Med. 151, 129–135. https://doi.org/10.1164/ajrccm.151.1.7812542.

14. WHO (2022). Global Tuberculosis Report 2022 (World Health Organization). https://www.who.int/teams/global-tuberculosis-programme/tb-reports/global-tuberculosis-report-2022/tb-disease-burden/2-2-tb-mortality.

15. Diedrich, C.R., and Flynn, J.L. (2011). HIV-1/mycobacterium tuberculosis coinfection immunology: how does HIV-1 exacerbate tuberculosis? Infect. Immun. 79, 1407–1417. https://doi.org/10.1128/iai.01126-10.

16. Báfica, A., Scanga, C.A., Schito, M.L., Hieny, S., and Sher, A. (2003). Cutting edge: in vivo induction of integrated HIV-1 expression by mycobacteria is critically dependent on Toll-like receptor 2. J. Immunol. 171, 1123–1127. https://doi.org/10.4049/jimmunol.171.3.1123.

17. Toossi, Z., Johnson, J.L., Kanost, R.A., Wu, M., Luzze, H., Peters, P., Okwera, A., Joloba, M., Mugyenyi, P., Mugerwa, R.D., et al. (2001). Increased replication of HIV-1 at sites of Mycobacterium tuberculosis infection: potential mechanisms of viral activation. J. Acquir. Immune Defic. Syndr. 28, 1–8. https://doi.org/10.1097/00042560-200109010-00001.

18. Lederman, M.M., Georges, D.L., Kusner, D.J., Mudido, P., Giam, C.Z., and Toossi, Z. (1994). Mycobacterium tuberculosis and its purified protein derivative activate expression of the human immunodeficiency virus. J. Acquir. Immune Defic. Syndr. 7, 727–733.

19. Zhang, Y., Nakata, K., Weiden, M., and Rom, W.N. (1995). Mycobacterium tuberculosis enhances human immunodeficiency virus-1 replication by transcriptional activation at the long terminal repeat. J. Clin. Invest. 95, 2324–2331. https://doi.org/10.1172/jci117924.

20. Bernier, R., Barbeau, B., Olivier, M., and Tremblay, M.J. (1998). Mycobacterium tuberculosis mannose-capped lipoarabinomannan can induce NF-kappaB-dependent activation of human immunodeficiency virus type 1 long terminal repeat in T cells. J. Gen. Virol. 79, 1353–1361. https://doi.org/10.1099/0022-1317-79-6-1353.

21. Souriant, S., Balboa, L., Dupont, M., Pingris, K., Kviatcovsky, D., Cougoule, C., Lastrucci, C., Bah, A., Gasser, R., Poincloux, R., et al. (2019). Tuberculosis Exacerbates HIV-1 Infection through IL-10/STAT3-Dependent Tunneling Nanotube Formation in Macrophages. Cell Rep. 26, 3586–3599.e7. https://doi.org/10.1016/j.celrep.2019.02.091.

22. Lastrucci, C., Bénard, A., Balboa, L., Pingris, K., Souriant, S., Poincloux, R., Al Saati, T., Rasolofo, V., González-Montaner, P., Inwentarz, S., et al. (2015). Tuberculosis is associated with expansion of a motile, permissive and immunomodulatory CD16(+) monocyte population via the IL-10/STAT3 axis. Cell Res. 25, 1333–1351. https://doi.org/10.1038/cr.2015.123.

23. Marin Franco, J.L., Genoula, M., Corral, D., Duette, G., Ferreyra, M., Maio, M., Dolotowicz, M.B., Aparicio-Trejo, O.E., Patino-Martinez, E., Charton, A., et al. (2020). Host-Derived Lipids from Tuberculous Pleurisy Impair Macrophage Microbicidal-Associated Metabolic Activity. Cell Rep. 33, 108547. https://doi.org/10.1016/j.celrep.2020.108547.

24. Dupont, M., Souriant, S., Balboa, L., Vu Manh, T.P., Pingris, K., Rousset, S., Cougoule, C., Rombouts, Y., Poincloux, R., Ben Neji, M., et al. (2020). Tuberculosis-associated IFN-I induces Siglec-1 on tunneling nanotubes and favors HIV-1 spread in macrophages. Elife 9, e52535. https://doi.org/10.7554/eLife.52535.

25. Goletti, D., Carrara, S., Vincenti, D., Giacomini, E., Fattorini, L., Garbuglia, A.R., Capobianchi, M.R., Alonzi, T., Fimia, G.M., Federico, M., et al. (2004). Inhibition of HIV-1 replication in monocyte-derived macrophages by Mycobacterium tuberculosis. J. Infect. Dis. 189, 624–633. https://doi.org/10.1086/381554.

26. Ranjbar, S., Boshoff, H.I., Mulder, A., Siddiqi, N., Rubin, E.J., and Goldfeld, A.E. (2009). HIV-1 replication is differentially regulated by distinct clinical strains of Mycobacterium tuberculosis. PLoS One 4, e6116. https://doi.org/10.1371/journal.pone.0006116.

27. Vorster, M.J., Allwood, B.W., Diacon, A.H., and Koegelenberg, C.F.N. (2015). Tuberculous pleural effusions: advances and controversies. J. Thorac. Dis. 7, 981–991. https://doi.org/10.3978/j.issn.2072-1439.2015.02.18.

28. Ferrer, J. (1997). Pleural tuberculosis. Eur. Respir. J. 10, 942–947.

29. Collins, K.R., Quiñones-Mateu, M.E., Wu, M., Luzze, H., Johnson, J.L., Hirsch, C., Toossi, Z., and Arts, E.J. (2002). Human immunodeficiency virus type 1 (HIV-1) quasispecies at the sites of Mycobacterium tuberculosis infection contribute to systemic HIV-1 heterogeneity. J. Virol. 76, 1697–1706. https://doi.org/10.1128/jvi.76.4.1697-1706.2002.

30. Toossi, Z. (2003). Virological and immunological impact of tuberculosis on human immunodeficiency virus type 1 disease. J. Infect. Dis. 188, 1146–1155. https://doi.org/10.1086/378676.

31. Lawn, S.D., Pisell, T.L., Hirsch, C.S., Wu, M., Butera, S.T., and Toossi, Z. (2001). Anatomically compartmentalized human immunodeficiency virus replication in HLA-DR+ cells and CD14+ macrophages at the site of pleural tuberculosis coinfection. J. Infect. Dis. 184, 1127–1133. https://doi.org/10.1086/323649.

32. Genoula, M., Marín Franco, J.L., Dupont, M., Kviatcovsky, D., Milillo, A., Schierloh, P., Moraña, E.J., Poggi, S., Palmero, D., Mata-Espinosa, D., et al. (2018). Formation of Foamy Macrophages by Tuberculous Pleural Effusions Is Triggered by the Interleukin-10/Signal Transducer and Activator of Transcription 3 Axis through ACAT Upregulation. Front. Immunol. 9, 459. https://doi.org/10.3389/fimmu.2018.00459.

33. Cavrois, M., De Noronha, C., and Greene, W.C. (2002). A sensitive and specific enzyme-based assay detecting HIV-1 virion fusion in primary T lymphocytes. Nat. Biotechnol. 20, 1151–1154. https://doi.org/10.1038/nbt745.

34. Cavrois, M., Neidleman, J., and Greene, W.C. (2014). HIV-1 Fusion Assay. Bio. Protoc. 4, e1212. https://doi.org/10.21769/BioProtoc.1212.

35. Stevenson, M., Stanwick, T.L., Dempsey, M.P., and Lamonica, C.A. (1990). HIV-1 replication is controlled at the level of T cell activation and proviral integration. EMBO J. 9, 1551–1560. https://doi.org/10.1002/j.1460-2075.1990.tb08274.x.

36. Clerc, I., Moussa, D.A., Vahlas, Z., Tardito, S., Oburoglu, L., Hope, T.J., Sitbon, M., Dardalhon, V., Mongellaz, C., and Taylor, N. (2019). Entry of glucose- and glutamine-derived carbons into the citric acid cycle supports early steps of HIV-1 infection in CD4 T cells. Nat. Metab. 1, 717–730. https://doi.org/10.1038/s42255-019-0084-1.

37. Valle-Casuso, J.C., Angin, M., Volant, S., Passaes, C., Monceaux, V., Mikhailova, A., Bourdic, K., Avettand-Fenoel, V., Boufassa, F., Sitbon, M., et al. (2019). Cellular Metabolism Is a Major Determinant of HIV-1 Reservoir Seeding in CD4(+) T Cells and Offers an Opportunity to Tackle Infection. Cell Metabol. 29, 611–626.e5. https://doi.org/10.1016/j.cmet.2018.11.015.

38. Hegedus, A., Kavanagh Williamson, M., and Huthoff, H. (2014). HIV-1 pathogenicity and virion production are dependent on the metabolic phenotype of activated CD4+ T cells. Retrovirology 11, 98. https://doi.org/10.1186/s12977-014-0098-4.

39. Duette, G., Pereyra Gerber, P., Rubione, J., Perez, P.S., Landay, A.L., Crowe, S.M., Liao, Z., Witwer, K.W., Holgado, M.P., Salido, J., et al. (2018). Induction of HIF-1α by HIV-1 Infection in CD4+ T Cells Promotes Viral Replication and Drives Extracellular Vesicle-Mediated Inflammation. mBio 9, e00757-18. https://doi.org/10.1128/mBio.00757-18.

40. Kumar, A., Abbas, W., and Herbein, G. (2013). TNF and TNF receptor superfamily members in HIV infection: new cellular targets for therapy? Mediat. Inflamm. 2013, 484378. https://doi.org/10.1155/2013/484378.

41. Yang, X., Chen, Y., and Gabuzda, D. (1999). ERK MAP kinase links cytokine signals to activation of latent HIV-1 infection by stimulating a cooperative interaction of AP-1 and NF-kappaB. J. Biol. Chem. 274, 27981–27988. https://doi.org/10.1074/jbc.274.39.27981.

42. Bosque, A., Nilson, K.A., Macedo, A.B., Spivak, A.M., Archin, N.M., Van Wagoner, R.M., Martins, L.J., Novis, C.L., Szaniawski, M.A., Ireland, C.M., et al. (2017). Benzotriazoles Reactivate Latent HIV-1 through Inactivation of STAT5 SUMOylation. Cell Rep. 18, 1324–1334. https://doi.org/10.1016/j.celrep.2017.01.022.

43. Gavegnano, C., Brehm, J.H., Dupuy, F.P., Talla, A., Ribeiro, S.P., Kulpa, D.A., Cameron, C., Santos, S., Hurwitz, S.J., Marconi, V.C., et al. (2017). Novel mechanisms to inhibit HIV reservoir seeding using Jak inhibitors. PLoS Pathog. 13, e1006740. https://doi.org/10.1371/journal.ppat.1006740.

44. Chan, J.K.L., and Greene, W.C. (2011). NF-κB/Rel: agonist and antagonist roles in HIV-1 latency. Curr. Opin. HIV AIDS 6, 12–18. https://doi.org/10.1097/COH.0b013e32834124fd.

45. Tong, O., Duette, G., O'Neil, T.R., Royle, C.M., Rana, H., Johnson, B., Popovic, N., Dervish, S., Brouwer, M.A.E., Baharlou, H., et al. (2021). Plasmacytoid dendritic cells have divergent effects on HIV infection of initial target cells and induce a pro-retention phenotype. PLoS Pathog. 17, e1009522. https://doi.org/10.1371/journal.ppat.1009522.

46. Van der Sluis, R.M., Zerbato, J.M., Rhodes, J.W., Pascoe, R.D., Solomon, A., Kumar, N.A., Dantanarayana, A.I., Tennakoon, S., Dufloo, J., McMahon, J., et al. (2020). Diverse effects of interferon alpha on the establishment and

reversal of HIV latency. PLoS Pathog. *16*, e1008151. https://doi.org/10.1371/journal.ppat.1008151.

47. Mutascio, S., Mota, T., Franchitti, L., Sharma, A.A., Willemse, A., Bergstresser, S.N., Wang, H., Statzu, M., Tharp, G.K., Weiler, J., et al. (2023). CD8(+) T cells promote HIV latency by remodeling CD4(+) T cell metabolism to enhance their survival, quiescence, and stemness. Immunity *56*, 1132–1147.e6. https://doi.org/10.1016/j.immuni.2023.03.010.

48. Bergstresser, S., and Kulpa, D.A. (2022). TGF-beta Signaling Supports HIV Latency in a Memory CD4+ T Cell Based In Vitro Model. Methods Mol. Biol. *2407*, 69–79. https://doi.org/10.1007/978-1-0716-1871-4_6.

49. Samer, S., Thomas, Y., Arainga, M., Carter, C., Shirreff, L.M., Arif, M.S., Avita, J.M., Frank, I., McRaven, M.D., Thuruthiyil, C.T., et al. (2022). Blockade of TGF-beta signaling reactivates HIV-1/SIV reservoirs and immune responses in vivo. JCI Insight *7*, e162290. https://doi.org/10.1172/jci.insight.162290.

50. Huang, S.H., Ren, Y., Thomas, A.S., Chan, D., Mueller, S., Ward, A.R., Patel, S., Bollard, C.M., Cruz, C.R., Karandish, S., et al. (2018). Latent HIV reservoirs exhibit inherent resistance to elimination by CD8+ T cells. J. Clin. Invest. *128*, 876–889. https://doi.org/10.1172/JCI97555.

51. Badley, A.D., Sainski, A., Wightman, F., and Lewin, S.R. (2013). Altering cell death pathways as an approach to cure HIV infection. Cell Death Dis. *4*, e718. https://doi.org/10.1038/cddis.2013.248.

52. Cummins, N.W., and Badley, A.D. (2013). Anti-apoptotic mechanisms of HIV: lessons and novel approaches to curing HIV. Cell. Mol. Life Sci. *70*, 3355–3363. https://doi.org/10.1007/s00018-012-1239-3.

53. Fernandez Larrosa, P.N., Croci, D.O., Riva, D.A., Bibini, M., Luzzi, R., Saracco, M., Mersich, S.E., Rabinovich, G.A., and Martinez Peralta, L. (2008). Apoptosis resistance in HIV-1 persistently-infected cells is independent of active viral replication and involves modulation of the apoptotic mitochondrial pathway. Retrovirology *5*, 19. https://doi.org/10.1186/1742-4690-5-19.

54. Battivelli, E., Dahabieh, M.S., Abdel-Mohsen, M., Svensson, J.P., Tojal Da Silva, I., Cohn, L.B., Gramatica, A., Deeks, S., Greene, W.C., Pillai, S.K., and Verdin, E. (2018). Distinct chromatin functional states correlate with HIV latency reactivation in infected primary CD4(+) T cells. Elife *7*, e34655. https://doi.org/10.7554/eLife.34655.

55. Battivelli, E., and Verdin, E. (2018). HIV(GKO): A Tool to Assess HIV-1 Latency Reversal Agents in Human Primary CD4(+) T Cells. Bio. Protoc. *8*, e3050. https://doi.org/10.21769/bioprotoc.3050.

56. Kim, E.H., Manganaro, L., Schotsaert, M., Brown, B.D., Mulder, L.C.F., and Simon, V. (2022). Development of an HIV reporter virus that identifies latently infected CD4(+) T cells. Cell Rep. Methods *2*, 100238. https://doi.org/10.1016/j.crmeth.2022.100238.

57. Cai, J., Gao, H., Zhao, J., Hu, S., Liang, X., Yang, Y., Dai, Z., Hong, Z., and Deng, K. (2021). Infection with a newly designed dual fluorescent reporter HIV-1 effectively identifies latently infected CD4(+) T cells. Elife *10*, e63810. https://doi.org/10.7554/eLife.63810.

58. Demaison, C., Parsley, K., Brouns, G., Scherr, M., Battmer, K., Kinnon, C., Grez, M., and Thrasher, A.J. (2002). High-level transduction and gene expression in hematopoietic repopulating cells using a human immunodeficiency [correction of imunodeficiency] virus type 1-based lentiviral vector containing an internal spleen focus forming virus promoter. Hum. Gene Ther. *13*, 803–813. https://doi.org/10.1089/10430340252898984.

59. Matheson, N.J., Peden, A.A., and Lehner, P.J. (2014). Antibody-free magnetic cell sorting of genetically modified primary human CD4+ T cells by one-step streptavidin affinity purification. PLoS One *9*, e111437. https://doi.org/10.1371/journal.pone.0111437.

60. Dube, M., Bego, M.G., Paquay, C., and Cohen, E.A. (2010). Modulation of HIV-1-host interaction: role of the Vpu accessory protein. Retrovirology *7*, 114. https://doi.org/10.1186/1742-4690-7-114.

61. Mohammadi, P., Desfarges, S., Bartha, I., Joos, B., Zangger, N., Muñoz, M., Günthard, H.F., Beerenwinkel, N., Telenti, A., and Ciuffi, A. (2013). 24 Hours in the Life of HIV-1 in a T Cell Line. PLoS Pathog. *9*, e1003161. https://doi.org/10.1371/journal.ppat.1003161.

62. Pawlowski, A., Jansson, M., Sköld, M., Rottenberg, M.E., and Källenius, G. (2012). Tuberculosis and HIV co-infection. PLoS Pathog. *8*, e1002464. https://doi.org/10.1371/journal.ppat.1002464.

63. Esmail, H., Riou, C., Bruyn, E.D., Lai, R.P.J., Harley, Y.X.R., Meintjes, G., Wilkinson, K.A., and Wilkinson, R.J. (2018). The Immune Response to Mycobacterium tuberculosis in HIV-1-Coinfected Persons. Annu. Rev. Immunol. *36*, 603–638. https://doi.org/10.1146/annurev-immunol-042617-053420.

64. Genoula, M., Marín Franco, J.L., Maio, M., Dolotowicz, B., Ferreyra, M., Milillo, M.A., Mascarau, R., Moraña, E.J., Palmero, D., Matteo, M., et al. (2020). Fatty acid oxidation of alternatively activated macrophages prevents foam cell formation, but Mycobacterium tuberculosis counteracts this process via HIF-1α activation. PLoS Pathog. *16*, e1008929. https://doi.org/10.1371/journal.ppat.1008929.

65. Dupont, M., Rousset, S., Manh, T.P.V., Monard, S.C., Pingris, K., Souriant, S., Vahlas, Z., Velez, T., Poincloux, R., Maridonneau-Parini, I., 1st, et al. (2022). Dysregulation of the IFN-I signaling pathway by Mycobacterium tuberculosis leads to exacerbation of HIV-1 infection of macrophages. J. Leukoc. Biol. *112*, 1329–1342. https://doi.org/10.1002/JLB.4MA0422-730R.

66. Ranjbar, S., Jasenosky, L.D., Chow, N., and Goldfeld, A.E. (2012). Regulation of Mycobacterium tuberculosis-dependent HIV-1 transcription reveals a new role for NFAT5 in the toll-like receptor pathway. PLoS Pathog. *8*, e1002620. https://doi.org/10.1371/journal.ppat.1002620.

67. He, X., Eddy, J.J., Jacobson, K.R., Henderson, A.J., and Agosto, L.M. (2020). Enhanced Human Immunodeficiency Virus-1 Replication in CD4+ T Cells Derived From Individuals With Latent Mycobacterium tuberculosis Infection. J. Infect. Dis. *222*, 1550–1560. https://doi.org/10.1093/infdis/jiaa257.

68. Deshmane, S.L., Amini, S., Sen, S., Khalili, K., and Sawaya, B.E. (2011). Regulation of the HIV-1 promoter by HIF-1α and Vpr proteins. Virol. J. *8*, 477. https://doi.org/10.1186/1743-422X-8-477.

69. Deshmane, S.L., Mukerjee, R., Fan, S., Del Valle, L., Michiels, C., Sweet, T., Rom, I., Khalili, K., Rappaport, J., Amini, S., and Sawaya, B.E. (2009). Activation of the oxidative stress pathway by HIV-1 Vpr leads to induction of hypoxia-inducible factor 1alpha expression. J. Biol. Chem. *284*, 11364–11373. https://doi.org/10.1074/jbc.M809266200.

70. Palmer, C.S., Duette, G.A., Wagner, M.C.E., Henstridge, D.C., Saleh, S., Pereira, C., Zhou, J., Simar, D., Lewin, S.R., Ostrowski, M., et al. (2017). Metabolically active CD4+ T cells expressing Glut1 and OX40 preferentially harbor HIV during in vitro infection. FEBS Lett. *591*, 3319–3332. https://doi.org/10.1002/1873-3468.12843.

71. Palmer, C.S., Henstridge, D.C., Yu, D., Singh, A., Balderson, B., Duette, G., Cherry, C.L., Anzinger, J.J., Ostrowski, M., and Crowe, S.M. (2016). Emerging Role and Characterization of Immunometabolism: Relevance to HIV Pathogenesis, Serious Non-AIDS Events, and a Cure. J. Immunol. *196*, 4437–4444. https://doi.org/10.4049/jimmunol.1600120.

72. Li, Q., Li, L., Liu, Y., Fu, X., Qiao, D., Wang, H., Lao, S., Huang, F., and Wu, C. (2011). Pleural fluid from tuberculous pleurisy inhibits the functions of T cells and the differentiation of Th1 cells via immunosuppressive factors. Cell. Mol. Immunol. *8*, 172–180. https://doi.org/10.1038/cmi.2010.80.

73. Chetty, S., Govender, P., Zupkosky, J., Pillay, M., Ghebremichael, M., Moosa, M.Y.S., Ndung'u, T., Porichis, F., and Kasprowicz, V.O. (2015). Co-infection with Mycobacterium tuberculosis impairs HIV-Specific CD8+ and CD4+ T cell functionality. PLoS One *10*, e0118654. https://doi.org/10.1371/journal.pone.0118654.

74. Adeoye, B., Nakiyingi, L., Moreau, Y., Nankya, E., Olson, A.J., Zhang, M., Jacobson, K.R., Gupta, A., Manabe, Y.C., Hosseinipour, M.C., et al. (2023). Mycobacterium tuberculosis disease associates with higher HIV-1-specific antibody responses. iScience *26*, 106631. https://doi.org/10.1016/j.isci.2023.106631.

75. Tyagi, P., Pal, V.K., Agrawal, R., Singh, S., Srinivasan, S., and Singh, A. (2020). Mycobacterium tuberculosis Reactivates HIV-1 via Exosome-Mediated Resetting of Cellular Redox Potential and Bioenergetics. mBio *11*, e03293-19. https://doi.org/10.1128/mBio.03293-19.

76. Larson, E.C., Novis, C.L., Martins, L.J., Macedo, A.B., Kimball, K.E., Bosque, A., Planelles, V., and Barrows, L.R. (2017). Mycobacterium tuberculosis reactivates latent HIV-1 in T cells in vitro. PLoS One *12*, e0185162. https://doi.org/10.1371/journal.pone.0185162.

77. Olson, A., Ragan, E.J., Nakiyingi, L., Lin, N., Jacobson, K.R., Ellner, J.J., Manabe, Y.C., and Sagar, M. (2018). Brief Report: Pulmonary Tuberculosis Is Associated With Persistent Systemic Inflammation and Decreased HIV-1 Reservoir Markers in Coinfected Ugandans. J. Acquir. Immune Defic. Syndr. *79*, 407–411. https://doi.org/10.1097/QAI.0000000000001823.

78. Bradley, T., Ferrari, G., Haynes, B.F., Margolis, D.M., and Browne, E.P. (2018). Single-Cell Analysis of Quiescent HIV Infection Reveals Host Transcriptional Profiles that Regulate Proviral Latency. Cell Rep. *25*, 107–117.e3. https://doi.org/10.1016/j.celrep.2018.09.020.

79. Shytaj, I.L., Procopio, F.A., Tarek, M., Carlon-Andres, I., Tang, H.Y., Goldman, A.R., Munshi, M., Kumar Pal, V., Forcato, M., Sreeram, S., et al. (2021). Glycolysis downregulation is a hallmark of HIV-1 latency

and sensitizes infected cells to oxidative stress. EMBO Mol. Med. *13*, e13901. https://doi.org/10.15252/emmm.202013901.

80. Williams, S.A., and Greene, W.C. (2007). Regulation of HIV-1 latency by T-cell activation. Cytokine *39*, 63–74. https://doi.org/10.1016/j.cyto.2007.05.017.

81. He, Y., Yang, Z., Zhao, C.S., Xiao, Z., Gong, Y., Li, Y.Y., Chen, Y., Du, Y., Feng, D., Altman, A., and Li, Y. (2021). T-cell receptor (TCR) signaling promotes the assembly of RanBP2/RanGAP1-SUMO1/Ubc9 nuclear pore subcomplex via PKC-theta-mediated phosphorylation of RanGAP1. Elife *10*, e67123. https://doi.org/10.7554/eLife.67123.

82. Light, R.W. (2010). Update on tuberculous pleural effusion. Respirology *15*, 451–458. https://doi.org/10.1111/j.1440-1843.2010.01723.x.

83. Vandergeeten, C., Fromentin, R., Merlini, E., Lawani, M.B., DaFonseca, S., Bakeman, W., McNulty, A., Ramgopal, M., Michael, N., Kim, J.H., et al. (2014). Cross-clade ultrasensitive PCR-based assays to measure HIV persistence in large-cohort studies. J. Virol. *88*, 12385–12396. https://doi.org/10.1128/JVI.00609-14.

84. Dobin, A., Davis, C.A., Schlesinger, F., Drenkow, J., Zaleski, C., Jha, S., Batut, P., Chaisson, M., and Gingeras, T.R. (2013). STAR: ultrafast universal RNA-seq aligner. Bioinformatics *29*, 15–21. https://doi.org/10.1093/bioinformatics/bts635.

85. Ewels, P., Magnusson, M., Lundin, S., and Käller, M. (2016). MultiQC: summarize analysis results for multiple tools and samples in a single report. Bioinformatics *32*, 3047–3048. https://doi.org/10.1093/bioinformatics/btw354.

86. Team, R.D.C. (2010). R: A Language and Environment for Statistical Computing. (No Title).

87. Wickham, H., Averick, M., Bryan, J., Chang, W., McGowan, L., François, R., Grolemund, G., Hayes, A., Henry, L., Hester, J., et al. (2019). Welcome to the Tidyverse. J. Open Source Softw. *4*, 1686. https://doi.org/10.21105/joss.01686.

88. Robinson, M.D., McCarthy, D.J., and Smyth, G.K. (2010). edgeR: a Bioconductor package for differential expression analysis of digital gene expression data. Bioinformatics *26*, 139–140. https://doi.org/10.1093/bioinformatics/btp616.

89. Smyth, G.K. (2004). Linear models and empirical bayes methods for assessing differential expression in microarray experiments. Stat. Appl. Genet. Mol. Biol. *3*, Article3. https://doi.org/10.2202/1544-6115.1027.

90. Yu, G., Wang, L.G., Han, Y., and He, Q.Y. (2012). clusterProfiler: an R package for comparing biological themes among gene clusters. OMICS *16*, 284–287. https://doi.org/10.1089/omi.2011.0118.

91. Rubione, J., Pérez, P.S., Czernikier, A., Duette, G.A., Pereyra Gerber, F.P., Salido, J., Fabiano, M.P., Ghiglione, Y., Turk, G., Laufer, N., et al. (2022). A Dynamic Interplay of Circulating Extracellular Vesicles and Galectin-1 Reprograms Viral Latency during HIV-1 Infection. mBio *13*, e0061122. https://doi.org/10.1128/mbio.00611-22.

92. Pasternak, A.O., Adema, K.W., Bakker, M., Jurriaans, S., Berkhout, B., Cornelissen, M., and Lukashov, V.V. (2008). Highly sensitive methods based on seminested real-time reverse transcription-PCR for quantitation of human immunodeficiency virus type 1 unspliced and multiply spliced RNA and proviral DNA. J. Clin. Microbiol. *46*, 2206–2211. https://doi.org/10.1128/JCM.00055-08.

STAR★METHODS

KEY RESOURCES TABLE

REAGENT or RESOURCE	SOURCE	IDENTIFIER
Antibodies		
Mouse anti-p24-FITC	Beckman Coulter	Clone KC57; Cat#6604665; RRID: AB_1575987
Mouse anti-human CD4⁻ APC	BD Biosciences	Clone Leu3A/SK3; Cat#566915; RRID: AB_2739445
Mouse anti-human CD3-BV421	BD Biosciences	Clone SK7; Cat#563797; RRID: AB_2744383
T cell Transact	Miltenyi Biotec	N/A
Chemicals, peptides, and recombinant proteins		
Phorbol myristate acetate	Sigma	Cat#P1585-1MG
Recombinant human TNF-alpha	R&D Systems	Cat#10291-TA
JQ1	Selleck Chemicals	Cat#S7110
Vorinostat	Selleck Chemicals	Cat#S1047
PEP005	Tocris	Cat#4054
Critical commercial assays		
Taqman Fast Advanced Master Mix	ThermoFisher Scientific	Cat#4444556
Quantitect SYBR Green PCR Master Mix	Roche	Cat#204141
PureLink Genomic DNA Mini Kit	ThermoFisher Scientific	Cat#K182001
Xtreme Gene HP DNA Transfection Reagent	Sigma Aldrich	Cat#6366236001
pAdVAntage ™ Vector	Promega	Cat#E1711
CD4⁺ T Cell Isolation Kit, Human	Miltenyi Biotec	Cat#130096533
Experimental models: Cell lines		
J-Lat 10.6	NIH AIDS Reagent Program	RRID: CVCL_8281
J-Lat 6.3	NIH AIDS Reagent Program	RRID: CVCL_8280
Jurkat (E6-1)	NIH AIDS Reagent Program	RRID: CVCL_0065
HEK293T	American Type Culture Collection	RRID: CVCL_1926
Oligonucleotides		
	See Table S5	
Recombinant DNA		
Plasmid: HIV-1 NL4-3AD8ENV	NIH Reagent Program	ARP-11346
Plasmid: pHEF-VSVg	NIH Reagent Program	ARP-4693
Plasmid: pNL4-3-ΔEnv-EGFP	NIH Reagent Program	ARP-11100
Plasmid: pCMV4-BlaM-Vpr	Donated by Warner Greene	Addgene plasmid # 21950
Software and algorithms		
Graphpad	Prism	https://www.graphpad.com
FastQC	Babraham Bioinformatics	www.bioinformatics.babraham.ac.uk
Trim Galore	Babraham Bioinformatics	www.bioinformatics.babraham.ac.uk
R Statistical Environment	R Project	http://www.Rproject.org
Tidyverse	Hadley Wickham	https://www.tidyverse.org
EdgeR	Bioconductor	https://bioconductor.org/packages/release/bioc/html/edgeR.html
clusterProfiler	Bioconductor	https://bioconductor.org/packages/release/bioc/html/clusterProfiler.html

(Continued on next page)

Continued

REAGENT or RESOURCE	SOURCE	IDENTIFIER
FlowJo v10.8	BD	https://www.flowjo.com/solutions/flowjo
FACSDiva v8.0.3	BD Biosciences	https://www.bdbiosciences.com/en-au/products/software/instrument-software/bd-facsdiva-software
Deposited data		
Transcriptional profile of primary CD4+ T cells treated with TB-PE	NCBI Gene Expression Omnibus	GSE248986
Bulk RNA-seq Data	GEO	GSE248986

RESOURCE AVAILABILITY

Lead contact

Further information and requests for resources and reagents should be directed to and will be fulfilled by the Lead Contact, Dr Gabriel Duette (gabriel.duette@sydney.edu.au).

Materials availability

Materials used in this study are available via correspondence with the lead contact.

Data and code availability

- Bulk RNA-seq data reported in this paper have been deposited at GEO and are publicly available as of the date of publication. Accession numbers are listed in the key resources table.
- This paper does not report original code.
- Any additional information required to reanalyze the data reported in this paper is available from the lead contact upon request.

EXPERIMENTAL MODEL AND STUDY PARTICIPANT DETAILS

Ethical statement

This research was carried out in accordance with the Declaration of Helsinki (2013) of the World Medical Association. This study was approved by the institutional review boards at the Hospital F. J Muñiz (NIN-2601-19) and the Academia Nacional de Medicina de Buenos Aires (12554/17/X); Facultad de Medicina, Universidad de Buenos Aires (Buenos Aires, Argentina); and the Western Sydney Local Health District which includes the Westmead Institute for Medical Research (2022/PID00100 - 2022/ETH00092). Buffy coats from healthy donors were obtained from the Australian Red Cross Blood Service, Sydney, Australia. Written informed consent was obtained from all participants.

Participant cohort and clinical samples

Pleural effusions were obtained by therapeutic thoracentesis at the Hospital F. J Muñiz (Buenos Aires, Argentina). The TB pleurisy diagnosis was based on a positive Ziehl– Neelsen stain or Lowestein–Jensen culture from pleural effusions and/or histopathology of pleural biopsy. The diagnosis was further confirmed by an *Mtb*-induced IFN-γ response and an adenosine deaminase-positive test.[82] Exclusion criteria included a positive HIV-1 test, and the presence of concurrent infectious diseases or non-communicable conditions (cancer, diabetes, or steroid therapy). None of the patients had multidrug-resistant TB. Recruited patients who developed pleural effusion were divided in two groups according to their etiology (Table S1). The first group included 9 patients diagnosed with tuberculous pleural effusion (TB-PE), while the second group comprised 4 patients with transudates resulting from heart failure (HF-PE) (Table S1).

Pleural effusion samples

The pleural effusions were collected in heparin tubes and centrifuged at 300 g for 10 min at room temperature without brake. The cell-free supernatant was transferred into new plastic tubes, further centrifuged at 12,000 g for 10 min and aliquots were stored at −80°C. After diagnosis, pools were prepared by mixing equal amounts of individual PE derived from a specific etiology. The pools were decomplemented at 56°C for 30 min and filtered by 0.22 μm to remove remaining debris or residual bacteria.

For the experimental conditions where pleural effusion was included, 20% v/v PE was added to the cell culture. This concentration of PE was determined as optimal by our group in previous studies.[21,23,32,64]

Primary CD4+ T cells and cell lines

Peripheral blood mononuclear cells (PBMCs) were obtained by Ficoll-Hypaque density gradient centrifugation from buffy coats of healthy donors. CD4+ primary T cells were isolated and purified from PBMCs by negative selection using a CD4+ T cell isolation kit (Miltenyi Biotec). For HIV-1 infection, cells were stimulated and activated with anti-CD3/CD28 activating antibody cocktail (MiltenyiBiotec) for two days in

cRF10: RPMI (Lonza) supplemented with 10% fetal bovine serum (FBS, Gibco),1X GlutaMAX (Gibco), 100 U/ml penicillin (Gibco), 100 μg/mL streptomycin (Gibco), and 100 U/ml IL-2 (MiltenyiBiotec).

The J-Lat (clones 10.6 and 6.3) and Jurkat (E6-1) human CD4$^+$ T cell lines were obtained from the NIH AIDS Reagent Program, Division of AIDS (NIAID, NIH). Cells were cultured in RF10: RPMI (Lonza) supplemented with 10% fetal bovine serum (FBS, Gibco), 1X GlutaMAX (Gibco), 100 U/ml penicillin (Gibco) and 100 μg/mL streptomycin (Gibco). HEK 293T cells were obtained from the American Type Culture Collection (ATCC, CRL-11268) and cultured in DMEM (Lonza) supplemented with 10% fetal bovine serum (FBS, Gibco),1X GlutaMAX (Gibco), 100 U/ml penicillin (Gibco) and 100 μg/mL streptomycin (Gibco).

Plasmids and HIV-1 viral strains

The molecular clones HIV-1 NL4-3AD8ENV (HIV^{NL4-3}), pNL4-3-ΔEnv-EGFP and pHEF-VSVg were obtained through the NIH AIDS Reagent Program. The plasmids pCMV4-BlaM-Vpr, a gift from Warner Greene (Addgene plasmid # 21950), and pAdVAntage Vector (Promega) were used for the HIV-1 fusion assay.

Preparation of viral stocks

HIV^{NL4-3} and dual HIV-1 latency reporter viral stocks were produced by transfection of the corresponding vector (1 μg/well) in HEK 293T cells (3×10^5 cells per well in 6-well plates) using X-treme gene transfection reagent (Roche). Pseudotyping was achieved by co-transfecting pHEF-VSVg (400 ng/well). HIV^{NL4-3}/BlaM-Vpr viral stock was produced by co-transfecting HEK 293T cells (3×10^5 cells per well in 6-well plates) with 1 μg NL4-3AD8ENV, 100 ng pCMV4-BlaM-Vpr and 60 ng pAdVAntage Vector using X-treme gene transfection reagent (Roche). Supernatant was harvested at 48 and 72 h post-transfection, cleared by centrifugation at 1500g for 10 min, and frozen at −80°C. The virus stocks were titrated by infecting Jurkat cells and flow cytometry analysis of p24 or GFP expression 72 h post-infection.

METHOD DETAILS

HIV-1 infection

Isolated CD4+T cells (obtained as described above) were cultured at a concentration of 10^6 cells/ml in cRF10 in a 96 well U-bottom plate and incubated overnight with the corresponding HIV-1 stock at 37°C. Then, cells were washed 2 times with cRF10, and fresh cRF10 was added. When indicated, the proportion of HIV-1-infected cells was determined by intracellular staining of the viral protein Gag-p24 with a Mouse anti-p24-FITC antibody (clone KC57, Beckman Coulter).

Cells infected with the dual HIV-1 latency reporter were spinoculated by centrifugation at 2200 rpm for 90 min in the presence of 8 μg/mL Polybrene and then incubated overnight at 37°C.

Quantification of HIV-1 reverse transcripts

Total DNA was then extracted from HIV-1 infected cells at 6 h post-infection using the PureLink Genomic DNA Mini Kit (Thermo Fisher Scientific). Quantitative PCR for R-U5 and LTR-Gag transcripts was performed using the following primers:

R/U5 Fwd: 5′-GGCTAACTAGGGAACCCACTG-3′
R/U5 Rev: 5′-CTGCTAGAGATTTTCCACACTGAC-3′
LTR/Gag Fwd: 5′-TGTGTGCCCGTCTGTTGTGT-3′
LTR/Gag Rev: 5′-GAGTCCTGCGTCGAGAGAGC-3′
β2m Fwd: 5′-TGCTGTCTCCATGTTTGATGTATCT-3′
β2m Rev: 5′-TCTCTGCTCCCCACCTCTAAGT-3′

Quantitative PCR (qPCR) was performed using the Quantitect SYBR green PCR Master mix (Roche) with 10 ng of DNA and 0.5 μM primers in a final volume of 10 μL. DNA amplification was performed using the CFX96 Touch Real-Time PCR Detection System (Bio-Rad). Each sample was amplified in triplicate and relative expression was calculated by normalization to β2m.

Quantification of integrated HIV-1 DNA

HIV-1 infected CD4$^+$ T cells were lysed in DNA lysis buffer (DirectPCR Lysis Reagent, Viagen Biotech) containing 0.4 mg/mL of Proteinase K (Sigma-Aldrich, St Louis, MO, USA). Cell lysates were incubated in a heating shaker (Eppendorf ThermoMixer) at 56°C and 750rpm for 18 h. Proteinase K was inactivated by heating the digested sample at 95°C for 10 min. Integrated HIV-1 DNA was quantified by Quantitative PCR (qPCR) as previously described, with minor modifications.[6,45] The qPCR was performed using the TaqMan Fast Advanced Master Mix for qPCR (Thermo Fisher Scientific) with 5μL of cell lysate in a final volume of 25 μL. DNA amplification was performed using the CFX96 Touch Real-Time PCR Detection System (Bio-Rad). Each sample was amplified in duplicate and relative levels of integrated HIV-1 DNA were calculated by normalization to CD3. Quantitative PCR for integrated HIV and CD3 were performed using the following primers and probes as described in Vandergeeten et al.[83]:

ULF1: ATG CCA CGT AAG CGA AAC TCT GGG TCT CTC TDG TTA GAC
Alu1: TCC CAG CTA CTG GGG AGG CTG AGG
Alu2: GCC TCC CAA AGT GCT GGG ATT ACA G
Lambda T: ATG CCA CGT AAG CGA AAC T

UR2: CTG AGG GAT CTC TAG TTA CC
UHIV Taqman: LC640-CAC TCA GGG CAA GCT TTA TTG AGG C-BBQ
HCD3OUT5': ACT GAC ATG GAA CAG GGG AAG
HCD3OUT3': CCA GCT CTG AAG TAG GGA ACA TAT
HCD3IN5': GGC TAT CAT CTC TCT TCA AGG T
HCD3IN3': CCT CTC TTC AGC CAT TTA AGT A
CD3 TaqMan: LC640-AGC AGA GAA CAG TTA AGA GCC TCC AT-BBQ

HIV-1 fusion assay

HIV-1 fusion assay was adapted from Cavrois et al.[33] Briefly, cells were incubated for 4h with HIV[NL4-3]/BlaM-Vpr at 37°C. After incubation, cells were washed with CO_2 independent medium (Gibco) and incubated for 1 h with 100 μL of CCF2-AM loading solution (Thermo Fisher Scientific) at room temperature in the dark. Next, cells were washed once with CO_2 independent media and incubated overnight in 200 μL of development media (Thermo Fisher Scientific) at room temperature. CCF2-AM loading solution and development media were prepared in accordance with manufacturer's instructions.[34] After the overnight incubation, cells were washed 3 times with PBS and fixed in 1% paraformaldehyde (PFA) for 20 min at 4°C. After fixation, the cells were washed with PBS twice, resuspended in 200 μL PBS and acquired on a LSRFortessa Flow Cytometer. Enzymatic cleavage of CCF2 by Vpr-BlaM shifts the CCF2 fluorescence emission spectrum from 520nm to 447nm, indicating viral uptake.

Dual HIV-1 latency reporter

To generate the dual HIV-1 latency reporter vector, pNL4-3-ΔEnv-EGFP was digested with HpaI and XhoI. Then, a synthetic gene fragment containing the Spleen-forming focus virus promoter sequence followed by the iRFP670 protein-coding sequence (gBlock; Integrated DNA Technologies, IDT) was assembled with the gel-purified plasmid using the HiFi Assembly Master Mix (NEB, E5520) disrupting *nef* sequence (Δnef). The vector sequence was verified by Sanger sequencing (Source BioScience).

RNAseq library

Primary CD4^{+} T cells were obtained as described above. A group of isolated CD4^{+} T cells were activated using anti-CD3/CD28 antibodies in the presence or absence of TB-PE, and after 20 h, the cells were harvested to perform bulk RNAseq. RNA from CD4^{+} T cells (2x10^{6} cells per condition) was extracted by using the RNeasy Plus Mini kit (QIAGEN). Extracted total RNA was quantified using the Qubit broad range RNA assay, and RNA quality was assessed using the Agilent 4200 Tapestation system. Library preparation was performed using 400ng of total RNA as input and the Illumina stranded mRNA Prep kit. Short read sequencing was performed on the Novaseq 6000 platform where a minimum of 20 million paired-end 50bp reads per sample were generated.

RNAseq analysis

Library sequencing quality was determined using FastQC (Babraham Bioinformatics: www.bioinformatics.babraham.ac.uk/). Illumina adapter sequence and low quality read trimming (read pair removed if < 20 base pairs) was performed using Trim Galore (Babraham Bioinformatics). STAR[84] was used to align reads to human genome hg38 using ENSEMBL gene annotations as a guide. Read counts data corresponding to ENSEMBL gene annotations were generated and the STAR flag –quantMode GeneCounts. Multiqc[85] was used to verify quality metrics. All analyses were performed in the R Statistical Environment[86] (http://www.Rproject.org) with the Tidyverse package.[87] EdgeR was used to perform background correction and normalize count data by library size.[88] Differentially expressed gene analysis was determined using the QLFtest[89] (BH MTC $p < 0.05$). Gene lists were functionally annotated with Gene Ontology Biological Process (GO:BP) pathways (adjusted p value < 0.05) using the clusterProfiler package.[90]

In vitro reactivation of HIV-1

J-Lat cells, clones 10.6 and 6.3, were plated at a concentration of 3x10^{5} cell per well in a 96-well plate and stimulated with the indicated latency reversal agent (LRA) for 48 h. Each LRA was individually titrated in both J-Lat clones to determine the optimal experimental concentration. To reverse HIV-1 latency in J-Lat cells clone 10.6, 0.5 ng/mL phorbol myristate acetate (PMA), 0.05 ng/mL TNF-α, 5nM PEP005, 1μM JQ1 and 10μM Vorinostat were used. To reverse HIV-1 latency in J-Lat cells clone 6.3, 2 ng/mL PMA, 10 ng/mL TNF-α and 50nM PEP005 were used. JQ1 and Vorinostat were not used in J-Lat cells clone 6.3 due to the high cytotoxicity observed in this cell clone when these LRAs were titrated. Cell viability was determined by Live/Dead near-infrared (Invitrogen) staining and HIV-1 reactivation by quantifying GFP expression by flow cytometry.

Ex vivo reactivation of HIV-1

Ex vivo HIV-1 latency reversal was assessed as previously described.[91] Briefly, CD4^{+} T cells were isolated from 40 mL of peripheral blood from HIV-1-infected individuals on ART by immunodensity negative-selection using the RosetteSep Human CD4^{+} T cell Enrichment Cocktail (STEMCELL Technologies). Cells were plated at a concentration of 1-3x10^{6}/mL in RF10 and stimulated with 2 ng/mL PMA for 16 h when indicated. RNA was extracted by using the PureLink RNA minikit (Invitrogen) and reverse transcribed using the SuperScript III Reverse

Transcriptase (Invitrogen) following the manufacturer's recommendations. HIV-1 unspliced RNA (US-RNA) quantification as previously described.[92] Briefly, a heminested PCR was run for 15 cycles and a second amplification round was performed by quantitative real-time PCR for 40 cycles. US-RNA copy number was normalized to 18S RNA expression. Each sample was assessed in triplicate, and a non-reverse-transcribed control was used to detect DNA contamination.

Glycolysis and oxidative phosphorylation rate measurement

CD4$^+$ T cells were purified by magnetic isolation and stimulated with anti-CD3/CD28 antibodies in the presence or absence of TB-PE. After 24 h, the cells were cultured in RPMI-based Seahorse medium (Agilent) supplemented with 10 mM D-glucose, 1 mM pyruvate and 2 mM glutamine and plated in a Seahorse 24-well plate at a concentration of 7x10^5 cells/well. Proton efflux rate (PER) and oxygen consumption rate (OCR) were measured using a seahorse XFe24 analyzer. ATP production rates were measured using the Seahorse XF Real-Time ATP Rate Assay kit. Oligomycin, rotenone and antimycin A were added to quantify mitochondrial-derived and glycolysis-derived ATP production rate. OCR and PER values were normalized by calculating the cellular area per condition.

QUANTIFICATION AND STATISTICAL ANALYSIS

The experimental data was analyzed using Prism (GraphPad Software). Normality of the data was tested using the Kolmogorov-Smirnov test. Based on the normality test, either one-way ANOVA followed by the Tukey's HSD post-test or Kruskal–Wallis followed by Dunn's post-test were used for multiple comparison analyses and a Student's t test used to compare two conditions. A p-value less than 0.05 was considered significant.